Clean Energy and Sustainability

SCIEPublish

Review

Agricultural Waste Derived Biochar: Production, Characterisation, Environmental Applications and Critical Perspectives—A Review

Hitesh V. Vaghasiya, Palak J. Patel, Pradeep Verma and Khushbu G. Patel *

Department of Chemistry, Swaminarayan University, Kalol 382725, Gujarat, India; hiteshvaghasiya@swaminarayanuniversity.ac.in (H.V.V.); palakpatel@swaminarayanuniversity.ac.in (P.J.P.); deanscience@swaminarayanuniversity.ac.in (P.V.)

* Corresponding author. E-mail: patelkhushbug09@gmail.com (K.G.P.)

Received: 5 June 2026; Revised: 13 July 2026; Accepted: 8 September 2026; Available online: 22 September 2026

ABSTRACT: Worldwide generation of crop residues exceeds four billion tonnes per year, much of which is openly burnt or landfilled, with consequences for air quality, greenhouse-gas emissions, and soil organic matter. Thermochemical conversion of these residues to biochar offers a valorisation route with the potential to contribute simultaneously to water and soil remediation and to durable carbon storage. This structured narrative review consolidates progress on agricultural waste derived biochar (AWDB) reported between 2020 and 2026. Slow pyrolysis, fast pyrolysis, microwave-assisted pyrolysis, and hydrothermal carbonisation are compared in terms of operating conditions, yield, and product attributes. Activation routes (steam, CO_2, KOH, $ZnCl_2$, H_3PO_4) and post-synthetic modifications (heteroatom doping, metal impregnation, magnetic functionalisation) are evaluated against porosity, surface chemistry, and adsorbate selectivity. Applications span heavy-metal, dye, antibiotic, and CO_2 removal, together with soil amendment and carbon sequestration. Persistent limitations are identified, including over-reliance on equilibrium capacities, inconsistent test protocols, sparse multicomponent data and incomplete life-cycle accounting. The distinction between biochar, activated biochar, and biochar-derived activated carbon is applied consistently, and the safety profile of the material—residual pyrolysis organics, potentially toxic elements, release of impregnated metals, and management of pollutant-loaded spent adsorbent—is treated as integral to the assessment. Priorities are proposed for standardised evaluation, mechanism-guided synthesis, data-driven design, and techno-economic assessment.

Keywords: Biochar; Agricultural waste; Pyrolysis; Hydrothermal carbonisation; Activation; Adsorption; Heavy metals; CO_2 capture

1. Introduction

Global crop production yields approximately 4–5 billion tonnes of agricultural residues each year, a substantial fraction of which is disposed of through open-field burning, landfill, or uncontrolled

© 2026 The authors. This is an open access article under the Creative Commons Attribution 4.0 International License (https://creativecommons.org/licenses/by/4.0/).

decomposition [1,2]. These pathways contribute to particulate air pollution, greenhouse gas (GHG) emissions, and the depletion of soil carbon and nutrient stocks that could otherwise be recycled within productive cropping cycles [3]. The problem is particularly acute in South and Southeast Asia, where rice straw, wheat straw, and sugarcane bagasse dominate the residue mass and where seasonal burning is a recurring driver of regional air-quality episodes [4]. Valorisation of agricultural waste, therefore, sits at the intersection of circular-economy thinking, climate-mitigation commitments, and rural energy strategy.

Among the available valorisation routes, thermochemical conversion to biochar has attracted sustained scientific and policy interest over the past two decades [5,6]. Biochar can be defined as the solid residue that remains after heating biomass at moderate temperature in the absence of, or with a limited supply of, molecular oxygen; the resulting material is enriched in carbon, partly aromatised and contains a developed pore network and a tunable distribution of oxygen-containing surface groups [7,8]. The interest it has attracted derives from its multifunctional character: a single biomass-derived solid can serve concurrently as a soil amendment, a long-term carbon store, and an inexpensive sorbent for both aqueous and gas-phase contaminants [9].

Research output on agricultural waste–derived biochar (AWDB) has expanded sharply. Bibliometric analysis of the Web of Science Core Collection shows a continual rise in annual biochar publications since 2009, with the most pronounced growth in 2018–2022 and more than 13,000 records for 2022–2023 alone; agricultural residues form one of the principal feedstock categories [10]. The technology base has grown from conventional slow pyrolysis to fast pyrolysis, microwave-assisted pyrolysis, and hydrothermal carbonisation, each offering distinct trade-offs in energy demand, product distribution, and biochar properties [11,12]. Activation and post-synthetic modification—alkaline (KOH, NaOH), acidic (H_3PO_4), salt-mediated ($ZnCl_2$) activation, together with heteroatom doping using N, S, or P—have extended the operational envelope toward surface areas above 2000 $m^2 \cdot g^{-1}$ and tailored functional-group distributions [13,14]. Composite and hybrid systems, particularly magnetic biochars and biochar–clay hybrids, now occupy a prominent place in the literature [15,16].

Despite this rapid expansion, several recurring limitations are evident in the literature. The field remains capacity-driven, with maximum equilibrium adsorption values from single-solute Langmuir fits dominating the reported metrics; dynamic performance, breakthrough behaviour and multicomponent competition receive comparatively little attention [17,18]. Testing conditions—initial pollutant concentration, sorbent dose, pH, temperature, and contact time vary so widely across laboratories that cross-study comparisons are often unreliable. Mechanistic interpretations are frequently inferred from isotherm and kinetic fits without complementary spectroscopic or computational evidence, leading to overconfident claims of chemisorption, ion exchange, or π–π stacking [18,19]. The sustainability narrative that frames biochar as a low-cost, green technology is rarely supported by quantitative life-cycle or techno-economic analyses at the system scale.

Against this backdrop the present review pursues four aims: to consolidate developments in the production, activation and characterisation of AWDB published between 2020 and 2026 with emphasis on cereal straws, husks, bagasse, stalks and shells; to evaluate AWDB performance in heavy-metal, dye, pharmaceutical and CO_2 sorption together with soil amendment, nutrient dynamics and carbon sequestration; to assess the quality of the evidence on which performance claims rest, including the metrics used to express them; and to identify the methodological, safety and translational gaps that AWDB must close to mature into a deployable environmental technology. Section 1.1 describes the literature-identification approach and its limitations; Section 1.2 states the contribution of this review relative to recent AWDB reviews. Section 2 introduces feedstocks and production routes; Section 3 examines activation and modification strategies, including the terminological distinction between biochar and biochar-derived activated carbon; Section 4 surveys characterisation; Section 5 reviews environmental applications, including soil ecosystem services and nutrient dynamics; Section 6 discusses adsorption

mechanisms and modelling; Section 7 sets out critical perspectives, including safety and end-of-life management; and Section 8 highlights research priorities. Figure 1 provides a schematic overview of the AWDB value chain.

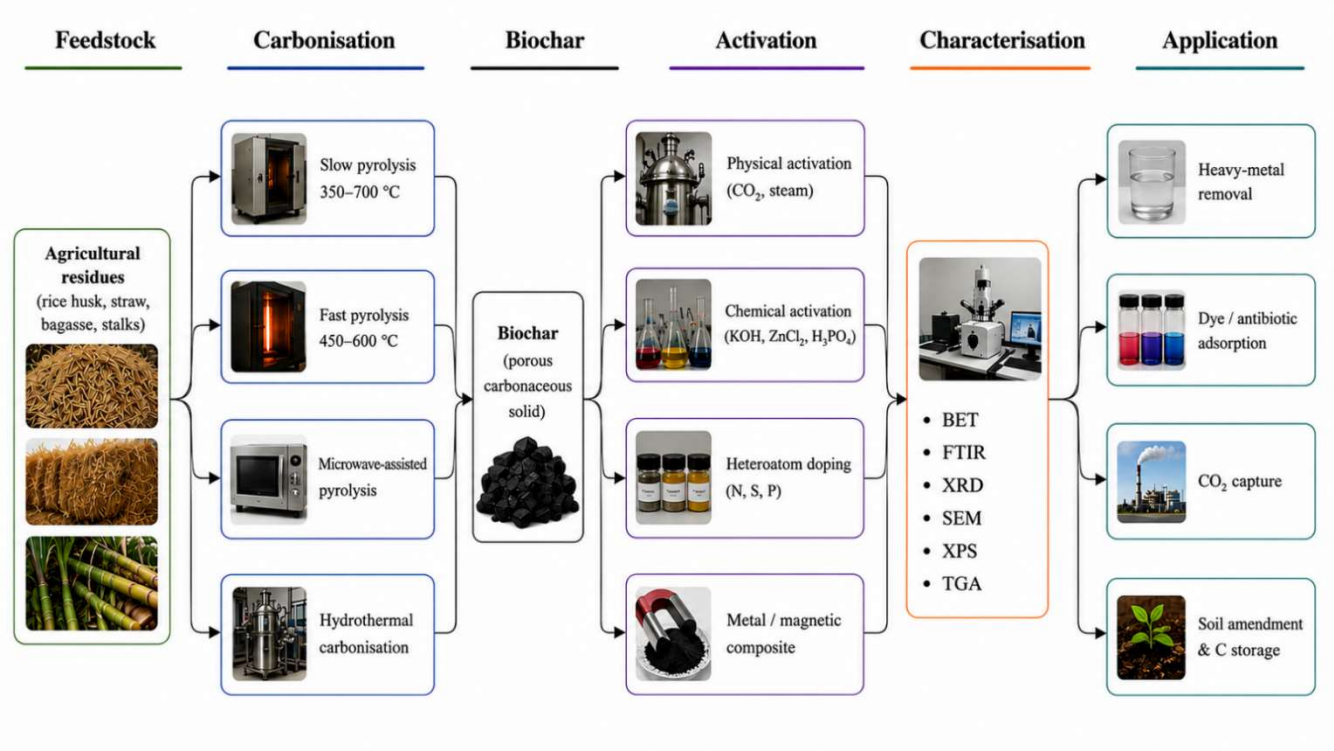


Figure 1. Conceptual overview of the agricultural waste–derived biochar (AWDB) value chain. Feedstock composition, the choice of carbonisation route, and the subsequent activation or modification step together determine pore architecture and surface chemistry, which in turn govern the suitability of the material for specific environmental applications. BET: Brunauer–Emmett–Teller; FTIR: Fourier-transform infrared; XRD: X-ray diffraction; SEM: Scanning electron microscopy; XPS: X-ray photoelectron spectroscopy; TGA: Thermogravimetric analysis.

1.1. Review Scope and Literature Identification

This article is presented as a structured narrative review rather than a systematic review or meta-analysis. The distinction is explicit because the heterogeneity of feedstocks, pyrolysis conditions, adsorbate systems, and reporting formats in the AWDB literature does not support quantitative pooling of effect sizes, and no pooled capacities or removal efficiencies are calculated. PRISMA 2020 [20] is used only as a transparency reference; because the review was not prospectively registered and a complete contemporaneous search and screening log was not retained, PRISMA-style record counts are not reported or reconstructed retrospectively.

Literature identification drew on the Web of Science Core Collection, Scopus, ScienceDirect, and PubMed, with Google Scholar used for forward citation checking and for locating relevant reports not readily identified in the primary databases. The literature-coverage window was defined as 1 January 2020 to 31 March 2026, with targeted use of older sources for foundational definitions, methods, and mechanisms. Exact database execution dates were not retained contemporaneously and are therefore not reported. Search concepts combined three blocks: (i) “biochar”, “hydrochar”, “pyrogenic carbon” or “biomass-derived carbon”; (ii) agricultural-residue terms including crop residue, rice husk, rice straw, wheat straw, sugarcane bagasse, corn stover, cotton stalk, groundnut shell and coconut shell; and (iii) application terms including adsorption, heavy metal, dye, antibiotic, CO_2 capture, soil amendment, carbon sequestration, life-cycle

assessment and techno-economic analysis. These terms were combined as appropriate for the syntax of each database and applied primarily to titles, abstracts, and keywords.

Selection was guided by the following eligibility framework. Priority was given to peer-reviewed English-language studies concerning lignocellulosic agricultural residues, either alone or in explicit comparison with other feedstocks, that reported relevant characterisation, processing, or performance information. Original experimental studies, review articles, meta-analyses, life-cycle assessments, and techno-economic analyses were considered where they contributed directly to the review aims. Conference abstracts, patents, and theses without accessible supporting data, studies dealing exclusively with unrelated non-agricultural feedstocks, and duplicate datasets were not used as the basis for quantitative claims. Where a numerical value could not be traced unambiguously to the retained manuscript notes or a cited source, it has not been reconstructed for this revision.

Candidate papers were assessed at the title/abstract and, where needed, full-text level during preparation and revision. A numerical screening cascade is not presented because the original working files do not contain a complete contemporaneous record of identification, deduplication, and exclusion counts. Likewise, the manuscript does not claim independent duplicate screening by two authors. The 101 references cited in the article constitute the documented bibliographic evidence base used for the narrative synthesis. This limitation is stated explicitly to avoid implying a level of systematic review reproducibility that cannot be supported by the retained records.

A defined set of pre-2020 sources has been retained deliberately. Definitions of biochar, the thermochemistry of lignocellulose decomposition, isotherm and kinetic formalisms, characterisation conventions, and the early soil-amendment literature cannot be sourced from the 2020–2026 window alone. These foundational references are used only for definitions, mechanisms, models, and methodological conventions; application-specific performance claims are supported by studies within the primary window, and where an older study is the best available support for such a claim, its age is stated in the text. Of the 101 references cited, 42 (41.6%) were published between 2020 and 2026, 29 (28.7%) between 2015 and 2019, 19 (18.8%) between 2010 and 2014, and 11 (10.9%) before 2010. Representative studies from the primary window are summarised in Section 5 by feedstock, processing condition, modification, application, reported performance, and principal limitation.

1.2. Contribution Relative to Recent Reviews

Biochar production, activation, water treatment, and soil amendment have each been reviewed extensively, and several recent reviews cover part of the ground addressed here [9,21–24]. The intended contribution of the present work is therefore not breadth of coverage but a critical, methodologically framed treatment of a deliberately narrow material class—biochar derived from lignocellulosic agricultural residues—organised around the synthesis–structure–function relationship and around the quality of the evidence supporting the performance claims made for it. Specifically, this review (i) reports a transparent literature-identification framework and explicitly states the limitations of the retained search record; (ii) treats the reporting metrics themselves as an object of analysis, including the limitations of the Langmuir q_m, the confounding of sorption with precipitation, and the inferential gap between kinetic-model fits and mechanism; (iii) applies a consistent distinction between biochar, activated biochar and biochar-derived activated carbon when comparing textural and CO_2-capture performance with commercial activated carbons; (iv) treats safety, contaminant leaching and end-of-life management of spent and metal-loaded biochars as part of the assessment; and (v) expresses standardisation and deployment-readiness requirements as testable reporting criteria rather than as general exhortations. Table 1 sets out this contribution against representative recent reviews.

Table 1. Contribution of the present review relative to representative reviews of biochar and biochar-based adsorbents. The comparison focuses on material scope and thematic emphasis; it does not make claims about the completeness of the search methods used by the cited reviews.

Sr. No.	Material Scope	Principal Emphasis	Additional Emphasis in the Present Review	Review [Ref.]
1.	Biochar, all feedstocks	Preparation, modification, and environmental application	Evidence-quality critique of adsorption metrics; agricultural-residue focus; safety and end-of-life	Wang & Wang (2019) [9]
2.	Biochar for aqueous heavy metals	Compilation of adsorption capacities	Multicomponent behaviour; precipitation artefacts; 2020–2026 evidence; soil ecosystem services	Inyang et al. (2016) [22]
3.	Modified biochar, heavy metals	Removal mechanisms	Standardised reporting; LCA/TEA; terminology; deployment readiness	Liu et al. (2022) [24]
4.	Crop-residue biochar	Production and life-cycle overview	Adsorption-metric quality; mechanism validation; contaminant leaching and disposal	Patel & Panwar (2023) [21]
5.	Modified biochar for dyes	Modification–performance mapping for dyes	CO_2 capture; soil nutrient dynamics; terminology; safety	Hama Aziz et al. (2024) [23]
6.	Lignocellulosic agricultural residues; structured narrative review	Synthesis–structure–function relationship and evidence quality across water, gas, and soil applications	Transparent scope and eligibility framework; reporting-metric critique; terminology; safety and end-of-life; deployment readiness	This review

Life cycle assessment (LCA), techno-economic analysis (TEA).

2. Agricultural Feedstocks and Biochar Production Routes

2.1. Composition and Availability of Agricultural Residues

Biochar properties are strongly governed by the composition of the parent biomass. Lignocellulosic agricultural residues are typically composed of cellulose (30–45 wt%), hemicellulose (20–35 wt%), and lignin (15–30 wt%), together with smaller fractions of extractives and inorganic ash [25,26]. Cellulose and hemicellulose decompose at relatively low temperatures (≈200–350 °C) and contribute mainly to volatile products and the early stages of pore development, while lignin—a thermally robust aromatic polymer—forms the carbon skeleton of the finished material [27]. Inorganic constituents such as silica, potassium, calcium and magnesium remain in the solid residue and may either enhance adsorption through additional ion-exchange capacity or hinder it by blocking pores and covering active sites [28].

Rice straw, rice husk, wheat straw, and sugarcane bagasse together account for the largest share of the global agricultural-residue mass, with the greatest volumes generated in China, India, and Southeast Asia [1,2]. Corn stover, cotton stalks, coconut shells, groundnut shells, and pulse residues contribute substantial further quantities. The combination of high availability with geographically concentrated and seasonal generation makes biochar production from agricultural waste particularly attractive for decentralised, rural-economy deployment.

Feedstock selection materially affects downstream behaviour. Rice husk, with silica content of 15–22 wt%, yields biochars in which embedded amorphous silica improves structural rigidity and provides additional cation-sorption sites. Wheat straw and rice straw deliver biochars with intermediate ash content (8–18 wt%) and a balanced population of oxygen-containing functional groups. Sugarcane bagasse, with low ash content (≈3–7 wt%) and high cellulose content, produces biochars with more uniform pore structures and higher carbon yields, which suits dye and pharmaceutical sorption [28]. Coconut and nut shells yield dense, microporous biochars traditionally favoured for gas-phase activated-carbon applications.

2.2. Slow, Fast, and Microwave-Assisted Pyrolysis

Slow pyrolysis remains the most widely used production route. It operates at 350–700 °C with heating rates of 5–20 °C·min^{-1} and residence times from minutes to hours under an inert atmosphere [29,30].

Biochar yields typically fall in the 25–40 wt% range on a dry feedstock basis, with the remainder distributed between bio-oil and non-condensable gases. Pyrolysis temperature exerts the strongest single influence on biochar properties. As temperature rises from 300 to 700 °C, biochar pH increases (from ≈7–8 to 9–11), fixed-carbon content rises (typically from 50–55% to 75–85%), volatile-matter content falls, and surface area increases substantially [31–33]. In a typical comparison, rice-husk biochar surface area increased from 64.8 $m^2 \cdot g^{-1}$ at 300 °C to 330.0 $m^2 \cdot g^{-1}$ at 700 °C, while the Langmuir capacity for Cd(II) rose in parallel from 4.15 to 58.5 to 67.7 $mg \cdot g^{-1}$ across the same 300–700 °C series [32], with simultaneous decreases in H/C and O/C atomic ratios reflecting progressive aromatisation. The increase in surface area is accompanied by a loss of oxygen-containing functional groups (–OH, –COOH, –C=O), which can compromise performance in metal-ion adsorption where surface complexation dominates. The optimum temperature is therefore application-dependent rather than universal.

Fast pyrolysis operates at higher heating rates (>100 $°C \cdot s^{-1}$) and shorter residence times (typically <2 s) at 450–600 °C [34]. It is optimised primarily for bio-oil production, with biochar as a co-product at 12–25 wt% of the feedstock. The resulting biochar usually exhibits lower fixed-carbon content and less developed porosity than slow-pyrolysis material, but its narrow particle-size distribution and uniform morphology can be advantageous in specific sorbent applications.

Microwave-assisted pyrolysis (MAP) offers volumetric heating and lower energy demand than conventional pyrolysis [12,35]. In MAP, electromagnetic energy at 2.45 GHz couples with polar species in the biomass to generate heat from within, eliminating the externally imposed thermal gradients of conventional reactors. For rice husk treated at 1000 W microwave power for 5 min, biochar surface areas of ≈170 $m^2 \cdot g^{-1}$ and pore volumes of 0.12 $cm^3 \cdot g^{-1}$ have been reported [35]. MAP typically delivers higher bio-oil and gas yields per unit input energy than conventional pyrolysis, although scale-up beyond pilot scale remains a challenge. Comparative energy claims for MAP should nonetheless be treated with caution: reported comparisons are made at laboratory or pilot scale, are rarely normalised to a common system boundary, and seldom include the electricity-generation efficiency upstream of the magnetron. The energy advantage of MAP is therefore best regarded as system- and scale-specific rather than as a general property of the route.

2.3. Hydrothermal Carbonisation

Hydrothermal carbonisation (HTC) processes wet biomass directly in sub-critical water at 180–250 °C and autogenous pressures of 10–40 bar [36,37]. The product, often termed hydrochar, is distinct from pyrolysis biochar: it generally has higher residual oxygen content, lower surface area, and higher hydrophilicity. Hydrochar is well-suited to feedstocks with moisture contents above 50 wt%—such as fruit-and-vegetable processing waste, food residues, sewage sludge, and post-harvest perishables—that would otherwise require energy-intensive drying. Downstream activation (steam, KOH, or CO_2) typically follows HTC to develop the porosity required for adsorption applications. Life-cycle and techno-economic analyses suggest that integrated HTC–activation routes can be competitive with conventional pyrolysis for wet residues, particularly when co-located with anaerobic digestion or other waste-management operations [38]. The available assessments are, however, few in number and differ in system boundary, feedstock cost, moisture assumption, and allocation method, so this comparison is case-specific and does not establish a general economic ranking of HTC against pyrolysis.

2.4. Comparative Summary

Table 2 summarises the principal characteristics of the four production routes. No single route is universally preferred: the choice depends on feedstock moisture, available infrastructure, and the intended biochar application. For dry cereal straws and husks, slow pyrolysis remains the dominant route in both

research and emerging commercial practice. For wet biomass and integrated waste-management settings, HTC offers compelling advantages despite the requirement for downstream activation.

Table 2. Comparative summary of biochar production routes for agricultural-waste valorisation. Values are indicative literature ranges rather than pooled estimates; the final column identifies the principal sources supporting each row.

Route	T (°C)	Heating Rate	Residence Time	Biochar Yield (wt%)	SSA ($m^2 \cdot g^{-1}$)	Typical Features	Suited Feedstocks	Ref.
Slow pyrolysis	350–700	5–20 °C·min^{-1}	min–h	25–40	<50 to 400	Balanced, well-developed pores; ash retained	Dry cereal straws, husks, bagasse	[29–33,39]
Fast pyrolysis	450–600	>100 °C·s^{-1}	<2 s	12–25	50–200	Lower fixed-C; uniform particle size	Pelletised straws, sawdust	[34]
Microwave-assisted (MAP)	300–600	Volumetric (instant)	5–30 min	20–35	100–250	Lower energy demand; pilot-scale only	Husks, cereal straws	[12,35]
Hydrothermal carbonisation	180–250	Autogenous pressure	1–6 h	40–60	5–20 (raw)	Higher O content; needs activation	Wet wastes, food residues, and sludge	[11,36–38]

3. Activation and Surface Modification Strategies

Untreated biochar from single-step pyrolysis often delivers limited performance because of moderate surface area, irregular pore structure, and incomplete development of surface functionality. Activation and post-synthetic modification, therefore, play a central role in transforming primary biochar into adsorbents suitable for specific environmental applications [13]. The choice of activation route depends on the target application, with no single route optimal for all cases.

3.1. Physical Activation

Physical activation uses gasifying agents, most commonly CO_2 or steam at 700–1000 °C to selectively burn off carbon and develop porosity. CO_2 activation tends to produce narrow micropores and is particularly effective for CO_2 capture, where pore widths below 0.7 nm are required for high-affinity uptake [40,41]. Steam activation produces a broader mix of micropores and mesopores, better suited to the adsorption of dyes and larger organic molecules. Both routes avoid the use of corrosive chemicals but require high-temperature operation, and the activation step typically consumes 30–50 wt% of the precursor biochar mass.

3.2. Chemical Activation

Chemical activation employs reactive agents, most commonly KOH, $ZnCl_2$ or H_3PO_4 at moderate temperatures (400–800 °C) to develop porosity and introduce specific functional groups. KOH activation produces very high surface areas (>2000 $m^2 \cdot g^{-1}$ are routinely reported; materials of this class are more accurately described as biochar-derived activated carbons, see Section 3.6) through reaction of K-containing intermediates with the carbon framework, yielding a tunable micropore network. The mechanism involves a complex sequence of solid-state reactions in which metallic potassium intercalates between graphitic layers, producing expanded porosity on washing [40,42].

$ZnCl_2$ activation is widely employed for the preparation of adsorbents targeting dyes and pharmaceuticals because of its tendency to yield mesoporous biochars with retained oxygen functionality at lower activation temperatures than KOH [23,43]. H_3PO_4 activation operates at the lowest temperatures (400–600 °C), introduces phosphate surface groups that enhance cation-exchange capacity, and is particularly used for the preparation of biochars targeting heavy metals and basic dyes. The recovery and recycling of these activating agents is operationally challenging, raising both environmental and economic concerns about large-scale chemical activation [14].

3.3. Heteroatom Doping and Surface Functionalisation

Beyond porosity, sorption selectivity is strongly governed by surface chemistry. Heteroatom doping introduces nitrogen, sulphur, phosphorus, or boron into the carbon framework, producing well-defined surface sites that interact selectively with target pollutants [44–47]. Nitrogen doping is the most widely studied modification. It can be implemented through co-pyrolysis with nitrogen-rich precursors (urea, melamine, dicyandiamide), through the use of intrinsically nitrogen-rich feedstocks, or through post-synthetic treatment with ammonia or nitrogen-containing acids. Nitrogen is incorporated into pyridinic, pyrrolic, graphitic, and amine configurations, as identified by X-ray photoelectron spectroscopy [47]. Pyridinic and pyrrolic nitrogen contribute basicity and act as Lewis-base sites that enhance CO_2 adsorption through acid–base interactions, while amine-type nitrogen provides chelation sites for heavy-metal ions [44,48]. Sulphur and phosphorus doping introduce thiol and phosphate groups that form strong interactions with soft heavy metals such as Hg^{2+} and Pb^{2+} through soft–soft acid–base principles. Oxygen functionalisation through HNO_3 or H_2O_2 treatment introduces carboxyl, hydroxyl, and carbonyl groups that enhance hydrogen bonding, raise surface polarity, and facilitate metal-ion complexation, although excessive oxidative treatment can collapse microporosity and degrade structural stability.

3.4. Metal Impregnation and Composite Biochars

Loading biochar with transition-metal species (Fe, Mn, Zn, Mg) or alkaline-earth metals (Ca) introduces additional sorption mechanisms, including surface complexation, chemisorption via carbonate formation, and Fenton-like catalytic activity. The most prominent class is magnetic biochar, in which iron-oxide nanoparticles (Fe_3O_4, γ-Fe_2O_3) are deposited onto the biochar matrix to enable rapid magnetic separation after sorption [16]. Magnetic biochars combine the high sorption capacity of carbonaceous adsorbents with the operational convenience of magnetic recovery, eliminating the filtration step that traditionally limits the practical use of fine-particle adsorbents in wastewater treatment [16]. Fe-modified pine-cone biochar has demonstrated strong adsorption of azithromycin and ciprofloxacin, with pseudo-second-order fits suggesting chemisorption involving ion exchange, complexation, and electrostatic interactions [49]. Other composites combine biochar with clay minerals (montmorillonite, bentonite), layered double hydroxides, or polymer coatings to introduce additional ion-exchange capacity or selective binding sites.

3.5. Matching Activation Strategy to Application

A central principle emerging from recent literature is that the activation strategy must be matched to the target application rather than pursued for maximum surface area alone. Table 3 summarises this relationship. For CO_2 capture, KOH activation paired with light nitrogen doping is the combination most frequently reported to perform well, although the published comparisons cover a limited set of activation conditions, and no optimum has been established across feedstocks. For dye and pharmaceutical sorption, $ZnCl_2$ or H_3PO_4 activation provides the mesoporosity and oxygen functionality required for accommodating bulky aromatic molecules. For heavy-metal removal, oxygen-rich, nitrogen-doped, or thiol-bearing biochars outperform purely high-surface-area materials. Although these structure–property–function relationships are widely reported, they remain underexploited in much of the published work, in which surface area is frequently cited as the primary performance metric without explicit linkage to the dominant sorption mechanism.

Table 3. Activation strategy, resulting biochar features, and recommended target applications. Temperature windows and features are indicative literature ranges; the final column identifies the principal sources supporting each row.

Sr. No.	Activation Route	Reagent/Agent	Temperature (°C)	Key Feature	Best-Suited Application	Sources
1.	Physical (CO_2)	CO_2 gas	700–1000	Narrow micropores	CO_2 capture	[13,40,41]
2.	Physical (steam)	Steam	700–1000	Broader meso/microporosity	Dyes, large organics	[13]
3.	Chemical (KOH)	KOH	600–800	Ultramicropores; SSA >2000 $m^2 \cdot g^{-1}$	CO_2 capture, gas adsorption	[14,40,42]
4.	Chemical ($ZnCl_2$)	$ZnCl_2$	450–700	Micro–meso balance; O-groups	Dyes, pharmaceuticals	[14,23,43]
5.	Chemical (H_3PO_4)	H_3PO_4	400–600	Mesopores; phosphate groups	Cationic metals, dyes	[14]
6.	N-doping	Urea, NH_3	300–800	Pyridinic/pyrrolic N	CO_2, heavy metals	[44–47]
7.	Magnetic (Fe-oxide)	$FeCl_3$/$FeSO_4$	300–500	Fe_3O_4 on carbon	Heavy metals, antibiotics	[16,49,50]

3.6. Biochar, Activated Biochar, and Biochar-Derived Activated Carbon

The term "biochar" is applied in the literature to materials that differ greatly in the extent to which the original carbonised structure has been reconstructed, and this obscures comparisons of textural and gas-capture performance. A material produced by single-step pyrolysis or hydrothermal carbonisation, retaining the ash and the anatomical structure of the feedstock and typically presenting surface areas below about 400 $m^2 \cdot g^{-1}$, is a different product from one subjected to KOH activation at 700–800 °C followed by acid washing, in which much of the ash has been removed and the carbon framework substantially rebuilt to give surface areas above 2000 $m^2 \cdot g^{-1}$. The latter is more accurately described as a biochar-derived activated carbon. The distinction matters in two places in particular: comparisons of specific surface area, where the two classes differ by an order of magnitude, and comparisons of CO_2-capture performance against commercial activated carbons, which are themselves chemically activated materials, so that a favourable comparison drawn between an aggressively activated biochar and a commercial activated carbon is not a comparison between biochar and activated carbon at all. Certification frameworks for biochar used in soil define the product primarily by feedstock, process, and carbon stability rather than by porosity [51,52], and materials that have undergone aggressive activation and washing generally fall outside their scope.

The following convention is used throughout this review. "Biochar" denotes the direct solid product of pyrolysis or HTC. "Activated biochar" denotes material subjected to mild physical or chemical activation that retains the essential character of the parent char, including a substantial part of its mineral fraction. "Biochar-derived activated carbon" denotes material produced by dedicated activation in which the ash has largely been removed and the porosity substantially reconstructed, typically presenting surface areas above about 1000 $m^2 \cdot g^{-1}$. Where a cited source does not provide enough information to make this assignment, the ambiguity is noted rather than resolved by assumption.

4. Physicochemical Characterisation

Reliable characterisation underpins both the interpretation of adsorption performance and the comparison of biochars across studies. Several complementary techniques are now standard.

4.1. Proximate and Ultimate Analysis

Proximate analysis quantifies moisture, volatile matter, fixed carbon, and ash, for which a modification of the standard coal method is required because of the high fixed-carbon content of biochars [53]; ultimate (elemental) analysis quantifies C, H, N, S, and O (by difference). The H/C and O/C atomic ratios indicate the degree of aromatisation and carbonisation, with low ratios (H/C < 0.4 and O/C < 0.2) commonly cited

as thresholds for biochar stability in soil and durable carbon storage [54,55]. These values are operational reporting conventions adopted in certification frameworks [51,52] rather than physical boundaries; measured stability also depends on soil mineralogy, climate, application depth, and the decay model used to extrapolate short incubations. Ash content varies widely across feedstocks (rice husk ≈ 20 wt%, sugarcane bagasse ≈ 3–7 wt%) and influences both the inherent surface area achievable and the effective adsorption capacity per unit mass of biochar.

4.2. Textural Analysis and Surface Chemistry

Brunauer–Emmett–Teller (BET) surface area [56], together with t-plot and NLDFT pore-size analyses, provides the textural fingerprint of the biochar. For strongly microporous chars, N_2 adsorption at 77 K underestimates the accessible micropore volume through diffusional limitation, and CO_2 adsorption at 273 K is the more reliable probe of pore widths below about 0.7 nm [57]. Specific surface areas of unmodified AWDB range from <50 to ≈400 $m^2 \cdot g^{-1}$, while activated and modified AWDB—including materials better described as biochar-derived activated carbons (Section 3.6)—span several hundred to >2500 $m^2 \cdot g^{-1}$ [13,14]. Fourier-transform infrared (FTIR) spectroscopy identifies surface functional groups: –OH (≈3400 cm^{-1}), aliphatic C–H (≈2900 cm^{-1}), C=O of carboxyls and ketones (≈1700 cm^{-1}), aromatic C=C (≈1600 cm^{-1}), and C–O of phenolic and ether groups (1000–1300 cm^{-1}). X-ray photoelectron spectroscopy (XPS) provides quantitative composition and detailed speciation of N, O, and S in modified biochars [47]. Boehm titration and zeta-potential measurements quantify acidic/basic surface groups and surface charge as a function of pH, both of which are essential for interpreting electrostatic contributions to adsorption.

4.3. Structural, Morphological, and Thermal Analysis

X-ray diffraction (XRD) reveals the degree of graphitic ordering and the presence of crystalline impurities such as silica, calcite, or iron oxides. Raman spectroscopy quantifies the intensity ratio of D (≈1350 cm^{-1}) to G (≈1580 cm^{-1}) bands as a measure of defect density relative to graphitic order, interpreted within the framework established for disordered and amorphous carbons [58]. Scanning (SEM) and transmission (TEM) electron microscopy reveal morphology, with feedstock-derived microstructures often preserved through carbonisation. Energy-dispersive X-ray spectroscopy (EDS) provides elemental mapping. Thermogravimetric analysis (TGA) under inert and oxidising atmospheres quantifies thermal stability and the partition between fixed and volatile carbon. CHN elemental analysis combined with TGA enables construction of the Van Krevelen diagram (H/C *vs*. O/C), which links carbonisation conditions to projected biochar stability in soil.

5. Environmental Applications

Table 4 summarises representative studies published within the primary review window, providing for each study the feedstock, the production conditions, the modification applied, the target application, the performance metric as reported in the source, and the principal limitation of the evidence. It is intended as an audit of the recent evidence base rather than a performance ranking: the entries were obtained under different conditions and are not directly comparable with one another, and the limitation column states the reason in each case.

Table 4. Representative agricultural-waste-derived biochar studies from the primary review window (2020–2026), classified by feedstock, processing condition, modification, application, reported performance metric, and principal limitation. Performance is reproduced as reported in the cited source and has not been normalised; entries are not mutually comparable.

Sr. No.	Feedstock	Production Condition	Modification	Application	Reported Performance	Principal Limitation of the Evidence	Ref.
1.	Rice husk	Slow pyrolysis, 300–700 °C	None	Cd(II), Se(IV) sorption	Langmuir q_m for Cd(II) rose from 4.15 to 58.5 to 67.7 mg·g^{-1} at 300, 500 and 700 °C; S_{BET} rose from 64.8 to 330.0 m^2·g^{-1} over the same range	Single-solute batch in deionised water; q_m extrapolated from fit	[32]
2.	Rice husk	Pyrolysis, 300–500 °C	HNO_3/KOH treatment	Heavy metals	Modified chars exceeded unmodified counterparts	Batch only; treatments compared at differing conditions	[39]
3.	Rice husk	Microwave, 1000 W, 5 min	None	Porosity development	SSA ≈ 170 m^2·g^{-1}; pore volume 0.12 cm^3·g^{-1}	Laboratory scale; specific energy consumption not reported on a common basis	[35]
4.	Sugarcane bagasse	Pyrolysis + chemical modification	$ZnCl_2$ activation, 600 °C	Methylene blue, acid red	MB 182 mg·g^{-1}; acid red 43 mg·g^{-1}	Freundlich fit; single solute; conditions differ from wastewater matrices	[28]
5.	Rice husk, wheat straw, corncob	Comparable pyrolysis conditions	None	Pb(II), Cd(II)	Removal 93.7–96.9% across the three feedstocks	Percentage removal at high dose and low C_0; not comparable across studies	[59]
6.	Sawdust (non-agricultural comparator)	Pyrolysis + co-precipitation	Magnetic Fe_3O_4	Pb(II)	RSM-optimised Pb(II) removal with magnetic recovery	Feedstock outside the AWDB class; batch only; regeneration and Fe release not quantified	[16]
7.	Coconut husk	Pyrolysis + Fe-oxide loading	Magnetic	Crystal violet	Removal above 90%	Batch, single solute; regeneration not reported	[50]
8.	Pine cone (non-agricultural comparator)	Pyrolysis + Fe modification	Fe	Azithromycin and ciprofloxacin	Effective uptake; PSO kinetics reported	Mechanism inferred from kinetic fits; feedstock outside the AWDB class	[49]
9.	Various agricultural residues	KOH activation	KOH	CO_2 capture	Uptake predicted from textural descriptors by machine learning	Model trained on heterogeneous literature data of variable quality	[60]
10.	Cellulose-derived carbon	Pyrolysis with doping	N/S doping	CO_2 capture	Uptake is enhanced relative to the undoped material	Model precursor rather than raw agricultural residue	[46]
11.	Food-waste digestate	Pyrolysis; TEA and LCA	None	Field application	Net greenhouse-gas benefit reported; economics boundary-dependent	Single case study; conclusions not generalisable across feedstocks	[38]
12.	Multiple feedstocks	Meta-analysis of published data	Various	Adsorption	Feedstock and pyrolysis temperature dominate property variance	Heterogeneous primary data; reporting inconsistencies propagate	[61]

5.1. Heavy-Metal Removal from Water

Surface- and ground-water contamination by toxic heavy metals—Pb^{2+}, Cd^{2+}, Cu^{2+}, Cr(VI), As(III)/As(V), Hg^{2+}, Ni^{2+}—remains a global environmental problem driven by mining, metallurgy, surface finishing, leather tanning, battery manufacturing, and electronic-waste processing. Conventional removal technologies (chemical precipitation, ion exchange, membrane filtration, and electrocoagulation) suffer

from high operating costs, secondary waste generation, or limited efficiency at low metal concentrations. Biochar-based adsorption offers a lower-cost, scalable alternative, with AWDB particularly attractive given the abundance of feedstocks and the waste-valorisation co-benefits [22].

Mechanisms of heavy-metal sorption on AWDB include electrostatic attraction, surface complexation with oxygen- and nitrogen-containing functional groups, cation exchange with alkaline-earth and alkali cations released from the ash phase, surface precipitation as carbonates or phosphates, and, for redox-active species such as Cr(VI), reduction followed by complexation of the reduced product [62,63]. The dominant mechanisms depend on the metal ion, biochar surface chemistry, and solution conditions, particularly pH. Pyrolysis temperature has a competing influence on metal adsorption: low-temperature biochars (300–500 °C) retain higher densities of oxygen-containing functional groups that favour Cd^{2+} and Pb^{2+} complexation, while high-temperature biochars (600–700 °C) develop greater surface area but reduced functional-group density [63]. Modification is therefore frequently used to combine the advantages of both regimes. Chemically modified cereal-residue biochars have repeatedly been reported to outperform their unmodified counterparts for Cd^{2+} and Pb^{2+} uptake; for rice-husk biochar, HNO_3 and KOH treatment raised capacities substantially, and the improvement was attributed to increased oxygen-containing surface functionality rather than to surface area alone [39,63]. Magnetic biochar–iron oxide composites have been optimised by response-surface methods for Pb^{2+} removal, with magnetic recovery replacing the filtration step; a Langmuir q_m of 504 $mg \cdot g^{-1}$ was reported at an adsorbent dose of 0.08 $g \cdot L^{-1}$, pH 7, an initial Pb^{2+} concentration of 50 $mg \cdot L^{-1}$ and a contact time of 10 min. The very low dose and the short contact time are worth noting, because a capacity expressed per unit mass rises as the dose falls, and a value obtained at 0.08 $g \cdot L^{-1}$ is not comparable with one obtained at the doses of 1–5 $g \cdot L^{-1}$ more typical of the studies surveyed here. The material in that study was, in addition, derived from sawdust rather than from an agricultural residue, and it is therefore treated throughout as a comparator rather than as an AWDB result [16].

Recent comparative studies confirm that feedstock selection materially affects metal-removal performance. Biochars from rice husk, wheat straw, and corncob, prepared under comparable pyrolysis conditions, achieved Pb^{2+} removal efficiencies of 96.4%, 95.4%, and 96.9%, respectively, with Cd^{2+} removal efficiencies of 94.7%, 93.7% and 95.8% [59]. Parallel comparative work has reinforced the strong dependence of metal-binding capacity on the starting biomass [64] and has shown how feedstock and pyrolysis temperature jointly control the properties that govern it, namely pH, ash and mineral content, surface functionality and surface area [65]. While such removal efficiencies are visually impressive, they are typically obtained at adsorbent doses and initial metal concentrations far from those encountered in real wastewater, a limitation discussed further in Section 7. For arsenic, present in solution predominantly as anionic As(III) and As(V), unmodified biochars perform poorly because of unfavourable electrostatic interactions. Iron-modified biochars, in which Fe_3O_4 or amorphous iron oxyhydroxides are deposited on the carbon surface, overcome this limitation by providing positively charged metal sites for arsenate complexation. Table 5 collects selected aqueous-phase results for heavy-metal and related contaminant sorption on agricultural-waste biochars. The table is laid out so that the experimental variables governing comparability are visible alongside each outcome: pyrolysis temperature, initial contaminant concentration, adsorbent dose, solution pH, contact time, and regeneration behaviour. Because the original source-by-source extraction workbook is unavailable, only outcomes that remain explicitly traceable in the retained notes and cited literature are reproduced, and every condition that the source publication does not report is marked NR rather than estimated, inferred, or silently omitted. Table 5 is therefore a qualitative evidence map rather than a cross-study benchmark, and the density of NR entries is itself a finding: it reflects the incomplete reporting of experimental conditions examined in Section 7.2, and it is the reason the tabulated outcomes cannot be used to rank materials or to infer relative adsorption capacity. Soil-application results, which are not comparable with aqueous adsorption data, are given separately in Table 6.

Table 5. Qualitative evidence map of reported aqueous-phase adsorption outcomes for agricultural-waste-derived biochars. The columns set out the experimental variables that determine whether results can be compared across studies: pyrolysis temperature, initial contaminant concentration (C_0), adsorbent dose, solution pH, contact time, and regeneration behaviour. Cells marked NR are not reported in the source publication or are not traceable in the retained notes; they are shown explicitly so that gaps in the primary literature remain visible to the reader rather than concealed by omission. Because the entries were obtained under different, largely undocumented conditions, they are not directly comparable and must not be read as a ranking of adsorbent performance. Conditions were re-extracted directly from the source publications wherever an accessible full text exists; values are reproduced as given there. NR = not reported or not retrievable; "Not studied" indicates that the source publication contains no regeneration experiment; q_m = maximum adsorption capacity from the fitted Langmuir isotherm. The two entries for reference [32] are the same material pyrolysed at different temperatures and are the only pair in the table that may legitimately be compared with one another.

Feedstock	Modification	Pyrolysis T (°C)	Adsorbate	C_0 (mg·L^{-1})	Dose (g·L^{-1})	pH	Contact Time	Reported Outcome	Regeneration	Ref.
Rice husk	Unmodified	NR	Pb^{2+}	NR	NR	5–6	NR	96.4% removal (batch)	NR	[59]
Wheat straw	Unmodified	NR	Cd^{2+}	NR	NR	6	NR	93.7% removal (batch)	NR	[59]
Corncob	Unmodified	NR	Pb^{2+}	NR	NR	5–6	NR	96.9% removal (batch)	NR	[59]
Rice husk	Unmodified	500	Cd^{2+}	10–500	2	7	6 h	58.5 mg·g^{-1} (Langmuir q_m, 25 °C)	Not studied	[32]
Rice husk	Unmodified	700	Cd^{2+}	10–500	2	7	6 h	67.7 mg·g^{-1} (Langmuir q_m, 25 °C)	Not studied	[32]
Sawdust (non-agricultural comparator)	Magnetic Fe_3O_4	NR	Pb^{2+}	50	0.08	7	10 min	504 mg·g^{-1} (Langmuir q_m; RSM-optimised)	NR	[16]
Coconut husk	Magnetic Fe-oxide	NR	Crystal violet	100	NR	NR	180 min (25 °C)	Removal > 90% (batch)	NR	[50]

Table 6. Selected soil-application results for agricultural-waste-derived and related biochars. These entries describe changes in bioavailability, nutrient status, or crop response and are not directly comparable with aqueous adsorption outcomes.

Feedstock	Modification	Soil/Crop System	Target	Reported Effect	Ref.
Sugarcane bagasse	Unmodified	Contaminated soil, mash bean	Cd, Cr	Reduced bioavailable fraction relative to the untreated control	[66]
Wheat and rice straw	Unmodified; differing pyrolysis temperatures	Calcareous soil, maize	N, P, K, and growth response	Nutrient dynamics and growth response depended on pyrolysis temperature	[67]
Various	Thiourea-modified	Acidic contaminated soil	Cd, Pb	Greater immobilisation than unmodified biochar, attributed to thiol/thioamide binding	[68]
Various (review synthesis)	Various	Contaminated soils	Pb, Cd, Cu, Zn	Bioavailable fractions are commonly reduced by 30–60%	[69]
Various (meta-analysis)	Various	Multiple crops and soils, field trials	Crop yield	Mean yield increases of 10–25% were concentrated on degraded, acidic, and sandy soils; near-zero responses were common on fertile temperate soils.	[70,71]

5.2. Adsorption of Organic Dyes

Synthetic dyes from textile, paper-pulp, leather, and food-processing effluents represent a major class of recalcitrant water pollutants. AWDB, particularly after chemical activation or magnetic functionalisation, has been widely investigated for dye removal. Maximum reported adsorption capacities span tens to several hundred mg·g^{-1} for cationic dyes such as methylene blue and crystal violet, and somewhat lower values for

anionic dyes such as methyl orange and Congo red, reflecting the prevailing negative surface charge of most biochars at near-neutral pH [43,72]. Key mechanisms include electrostatic attraction (driven by the pH-dependent surface charge), π–π stacking between aromatic adsorbate and graphitic biochar domains, hydrogen bonding between dye carbonyl/amine groups and biochar –OH/–COOH groups, and pore filling for small dye molecules [23]. $ZnCl_2$-activated sugarcane-bagasse biochar pyrolysed at 600 °C has been reported to take up 182 $mg \cdot g^{-1}$ of methylene blue and 43 $mg \cdot g^{-1}$ of acid red, the difference between the cationic and anionic dye reflecting the prevailing negative surface charge; in that study, the isotherms were better described by the Freundlich than the Langmuir model, indicating a heterogeneous surface [23,28]. Both figures were obtained in single-solute batch systems and are not transferable to dye-house effluent.

5.3. Adsorption of Antibiotics and Pharmaceutical Residues

Pharmaceutical contaminants in surface and ground waters, particularly antibiotics, are an emerging concern because of their role in driving antimicrobial resistance and their incomplete removal by conventional wastewater treatment, which acts as a route of release rather than a barrier [73]. AWDB has been investigated for the adsorption of a range of fluoroquinolone, sulphonamide, tetracycline, macrolide, and beta-lactam antibiotics [74,75]. Reported capacities for adsorbents derived from rice husk, wheat straw, corn straw, and shell biochars range from a few to several hundred $mg \cdot g^{-1}$, with the highest values reported for highly modified materials [76–78].

Sorption mechanisms are typically dominated by hydrogen bonding between antibiotic carbonyl, hydroxyl, and amine groups and oxygen-containing biochar surface groups, electrostatic interactions modulated by pH (antibiotics are typically zwitterionic with pKa values of ≈3–9), and π–π stacking between aromatic rings of the antibiotic and graphitic biochar domains [79]. Recent work has explored magnetic and metal-decorated biochars to enhance antibiotic capture; one example is a $NiFe_2O_4$–biochar composite that combines high antibiotic uptake with easy magnetic recovery [80]. Iron-modified pine-cone biochar has shown effective adsorption of azithromycin and ciprofloxacin under environmentally relevant conditions [49]. Even allowing for the constraints of laboratory batch experiments, the demonstrated capacities and mechanisms support AWDB as a viable component of antibiotic-removal systems for wastewater treatment plants and decentralised treatment units [81].

5.4. CO_2 Capture

Carbon dioxide capture from flue gases is a key element of climate-mitigation strategies. Biochar-derived adsorbents are attractive because they combine high stability, tunable porosity, and the co-benefit of carbon sequestration in the precursor biomass. Performance is governed by the surface chemistry of the biochar (particularly the density of basic sites) and the micropore-size distribution, with pores smaller than ≈0.7 nm being optimal for CO_2 adsorption at near-atmospheric pressures due to confinement and quadrupole interactions [82,83].

KOH-activated rice-husk biochar has achieved CO_2 uptakes of 4–6 $mmol \cdot g^{-1}$ at 1 bar and 25 °C, comparable to commercial activated carbons and zeolites [40,84–86]; the comparison is between two chemically activated materials rather than between biochar and activated carbon (Section 3.6). Nitrogen-doped biochars from agricultural residues, particularly those prepared via co-pyrolysis with urea or melamine, achieve enhanced CO_2 selectivity over N_2 through pyridinic and pyrrolic nitrogen sites that interact with CO_2 through acid–base mechanisms [44]. The relative roles of pore-size distribution and nitrogen functionality remain debated, with recent studies indicating that micropore volume in the 0.4–0.7 nm range is more predictive of CO_2 capacity than total nitrogen content [41].

5.5. Soil Amendment, Nutrient Dynamics, and Soil Ecosystem Services

Application of biochar to agricultural soils, historically inspired by the terra preta dark earths of Amazonia has been extensively investigated for its dual role in soil fertility improvement and long-term carbon sequestration [87]. AWDB derived from cereal straws, husks, and bagasse is particularly attractive because the residues are abundant, locally available, and otherwise often burned or landfilled. Biochar improves soil function through physical effects (water-holding capacity, aggregate stability, aeration), chemical effects (cation-exchange capacity, pH buffering for acidic soils, nutrient retention), and biological effects (enhanced microbial activity, mycorrhizal associations, reduced GHG emissions). Meta-analyses of field trials report average crop-yield increases of 10–25% following biochar application, with greater responses on degraded, acidic, or sandy soils than on already-fertile temperate soils [70,71]. These averages conceal wide variance: responses are conditional on soil type, texture, climate, application rate, and nutrient management, and neutral or negative yield responses are common on fertile temperate soils, so the range should be read as context-dependent rather than as a general expectation [71,88]. A representative analysis estimated that biochar application to Chinese farmland could increase soil organic carbon by 1.9 Pg C, reduce CH_4 and N_2O emissions by 25 and 20 Mt CO_2-eq year^{-1}, respectively, and increase crop yields by ≈19% under sustained application [89].

Nutrient dynamics are central to the agronomic value of AWDB, and the mechanisms involved differ from those governing aqueous adsorption. Cereal-straw and husk biochars carry appreciable K, Ca, and Mg in the ash fraction, much of which is released comparatively rapidly after application, whereas most feedstock N is volatilised during pyrolysis, and the N retained in the char is predominantly in heterocyclic forms of low short-term plant availability [67,88]. Phosphorus is largely retained in the solid, but its availability depends on ash chemistry and on the Ca, Fe, and Al content of both char and receiving soil. The more durable contribution of biochar to nutrient supply is indirect: retention of ammonium and of dissolved organic nutrients on oxidised surfaces, and within the organic coating that develops on aged biochar, reduces leaching losses and improves the synchrony between nutrient release and crop demand [88,90]. Reported effects on N_2O emission and on nitrification are variable in both direction and magnitude, and the conditions under which suppression occurs are not yet well defined.

Cation-exchange capacity and pH buffering are the soil-chemical functions most consistently attributed to AWDB. Oxidation of aromatic surfaces during ageing generates carboxyl and phenolic groups that raise Cation-exchange capacity (CEC) over months to years, so measurements on freshly produced material generally understate the CEC contribution of aged biochar in the field. The alkalinity of high-temperature cereal-residue biochars, deriving from carbonates and oxides in the ash, provides a liming effect that is valuable on acidic soils; the same property carries a risk of over-alkalinisation, induced Fe, Mn, and Zn deficiency, and clay dispersion on soils that are already neutral to alkaline or that are sodic [88]. Application rate and initial soil pH, therefore, need to be reported together for a soil result to be interpretable.

Biological responses are less predictable. Increases in microbial biomass, shifts in bacterial-to-fungal ratios, and stimulation of enzyme activities associated with C, N, and P cycling are frequently reported, and are usually attributed to habitat provision within the pore network, sorption of inhibitory compounds, and improved nutrient and water status. Opposite responses also occur, particularly where labile pyrolysis condensates, high salt loads, or residual polycyclic aromatic hydrocarbons are present in the applied material [88,91,92]. Because most of this evidence derives from short-term incubations and pot experiments, the persistence of microbial and enzymatic responses under field conditions remains poorly constrained.

Physical effects include increases in plant-available water capacity, reductions in bulk density, and improvements in aggregate stability. These are most pronounced in coarse-textured and degraded soils and are frequently negligible in well-structured loams. They also scale with application rate, which is one reason

why the doses commonly used in pot experiments—often 1–5% *w*/*w*, equivalent to very large field rates—do not translate directly into agronomic practice.

A recurring weakness in the soil-amendment literature is the imbalance between pot and field evidence. Pot studies dominate, use high application rates, disturbed soils, and short durations, and systematically report larger effects than field trials of comparable materials. Crop responses are species- and system-specific: cereals on acidic or sandy tropical soils show the largest and most reproducible yield gains, whereas responses in temperate cereal and vegetable systems are frequently neutral [70,71,88]. Interactions with other inputs matter as much as the properties of the biochar itself. Co-application with mineral fertiliser, compost, or manure generally produces larger and more consistent responses than biochar alone, which is consistent with the interpretation that AWDB supplies retention capacity rather than nutrients; interactions with irrigation regime determine whether any water-retention benefit is expressed at all. Agronomic recommendations for AWDB accordingly require site-specific evaluation, multi-season field trials, and reporting of soil type, texture, initial pH, nutrient status, application rate, and co-applied inputs. A recent synthesis of biochar effects on soil ecosystem services and nutrient dynamics provides a usable framework for such reporting [88]. Risks specific to soil application, salinity, and ash loading from K-rich cereal-residue chars, transfer of potentially toxic elements accumulated in the feedstock, residual pyrolysis organics, and over-liming are considered together with end-of-life issues in Section 7.5. Representative soil-application results are collected in Table 6.

5.6. Carbon Sequestration, Stability, and Contaminated-Soil Remediation

The carbon sequestration potential of biochar depends on its thermal and biological stability. The frequently quoted figure that approximately 50% of feedstock carbon is retained in stable aromatic form, with mean residence times in soil of 100–1000 years, is an order-of-magnitude generalisation drawn from a heterogeneous body of incubation and modelling studies [54,55]. Retained fraction and residence time both vary with feedstock, pyrolysis temperature, soil mineralogy, and climate, and centennial estimates obtained by extrapolating from short incubations carry substantial, rarely quantified uncertainty. The most stable biochars are those produced at higher temperatures (>500 °C) with low H/C and O/C ratios. Recent life-cycle assessments of agricultural-residue biochar systems indicate net GHG removals of 0.7–2.5 t CO_2-eq per tonne of biochar applied, depending on feedstock, production technology, and reference baseline [38,54,93]. Beyond agricultural use, biochar application has been investigated for the remediation of heavy-metal-contaminated soils: the combination of high cation-exchange capacity, oxygen-functional-group complexation, and pH buffering reduces the bioavailable fractions of Pb, Cd, Cu, and Zn in contaminated soils, with reductions of 30–60% commonly reported for typical application rates of 1–5% *w*/*w* [69]. Surface-functionalised biochars carrying sulphur ligands, such as thiourea-modified materials, have been shown to immobilise Cd and Pb in acidic soils more effectively than unmodified biochars through soft–soft acid–base interactions with thiol/thioamide groups [68].

6. Adsorption Mechanisms, Kinetics, and Isotherms

6.1. Classes of Interaction

Adsorption on AWDB rarely proceeds through a single mechanism. The dominant interactions, summarised schematically in Figure 2, can be grouped as: (i) electrostatic attraction between charged adsorbate species and the oppositely charged biochar surface; (ii) surface complexation, in which inner-sphere coordination bonds form between metal cations and surface O- or N-containing functional groups—the dominant mechanism for Pb^{2+} and Cd^{2+} on oxygen-rich biochars; (iii) ion exchange, in which alkali and alkaline-earth cations (K^+, Na^+, Ca^{2+}, Mg^{2+}) on the biochar surface are displaced by target heavy-metal cations; (iv) cation–π and π–π interactions between aromatic pollutant rings and graphitic carbon domains,

especially relevant for aromatic dyes and pharmaceuticals; (v) hydrogen bonding between –OH, –NH or carbonyl groups on the biochar surface and donor/acceptor sites on the adsorbate; (vi) hydrophobic interactions between non-polar adsorbate moieties and hydrophobic biochar surfaces; (vii) pore filling, with confined adsorbates benefiting from enhanced van der Waals interactions through pore-wall overlap; (viii) precipitation of insoluble hydroxides, carbonates or phosphates at the biochar surface under near-neutral or alkaline pH; and (ix) redox reactions, notably the reduction of Cr(VI) to Cr(III) by electron-donating biochar surface groups. For most adsorbate–adsorbent systems, several of these mechanisms operate in parallel, with their relative contributions varying with pH, ionic strength, temperature, and adsorbate concentration. Robust mechanistic identification, therefore, requires multi-technique evidence rather than reliance on a single isotherm or kinetic fit [24].

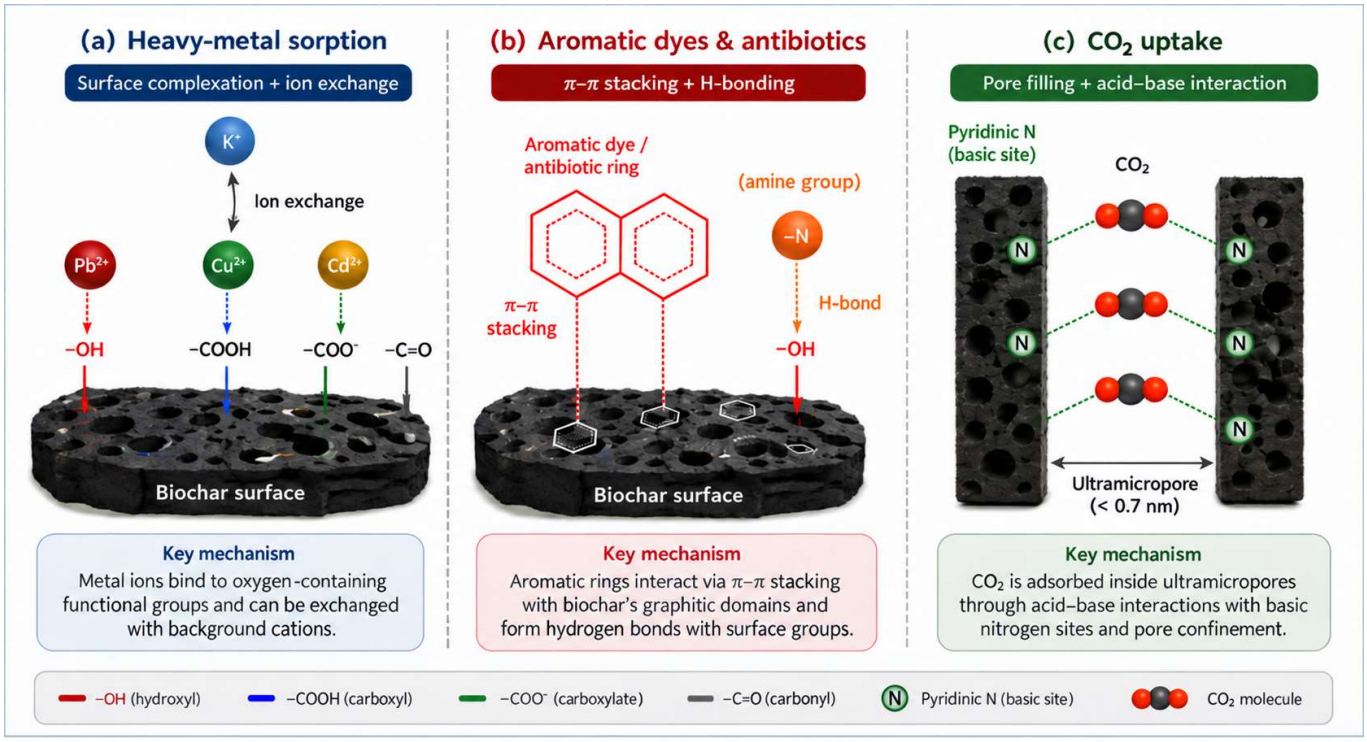


Figure 2. Schematic of the dominant interaction modes between aqueous- and gas-phase pollutants and the surface of agricultural waste–derived biochars. Surface complexation with oxygen-containing groups dominates for divalent heavy metals; π–π stacking and hydrogen bonding govern aromatic organics and antibiotics; ultramicropore filling combined with quadrupole interactions controls CO_2 uptake.

6.2. Equilibrium Isotherms

Equilibrium isotherms describe the relationship between residual adsorbate concentration (C_e) and equilibrium adsorption capacity (q_e). The Langmuir model assumes monolayer adsorption on a homogeneous surface with energetically equivalent sites and no lateral interactions; agreement with the Langmuir form does not by itself confirm any of these assumptions [18]. The Freundlich model is empirical, accommodating surface heterogeneity through a power-law relationship but providing no theoretical saturation limit. The Temkin model introduces a linear decrease in adsorption enthalpy with surface coverage, while the Redlich–Peterson and Sips models combine elements of Langmuir and Freundlich behaviour through additional fitting parameters. Comprehensive treatments of these and related two- and three-parameter isotherm forms, together with guidance on the assumptions implicit in each, have been compiled elsewhere [94]. A common methodological problem in the AWDB literature is the practice of comparing maximum capacities (q_m) derived from Langmuir fits across studies in which the experimental

concentration ranges were very different. Because q_m is an asymptotic value obtained by mathematical extrapolation, its reliability declines rapidly when the fitted equilibrium concentrations approach or exceed those used experimentally [18,95]. Widespread reporting of q_m values without explicit indication of the experimental concentration range is a persistent source of misleading comparisons.

6.3. Kinetic and Thermodynamic Modelling

The pseudo-first-order (PFO) and pseudo-second-order (PSO) kinetic models dominate descriptions of adsorption kinetics. The PSO model is typically reported as providing better correlation with experimental data, an observation often interpreted as evidence of chemisorption. This mechanistic conclusion is, however, frequently overstated: the greater mathematical flexibility of PSO particularly its ability to accommodate long approach-to-equilibrium tails, provides a better fit across wider time scales than PFO regardless of the underlying mechanism [19,96]. The Elovich model and the Weber–Morris intraparticle-diffusion model provide additional kinetic descriptions, the latter being particularly useful for identifying multiple rate-controlling steps. A linear Weber–Morris plot that does not pass through the origin indicates that intraparticle diffusion is not the sole rate-limiting step [97].

Thermodynamic parameters such as Gibbs free-energy change ($\Delta G°$), enthalpy change ($\Delta H°$), and entropy change ($\Delta S°$) are commonly calculated to evaluate adsorption feasibility and to distinguish between physisorption and chemisorption regimes. Adsorption enthalpies below ≈40 $kJ \cdot mol^{-1}$ are typically associated with physisorption, while values above ≈80 $kJ \cdot mol^{-1}$ are associated with chemisorption involving stronger chemical bonding. Intermediate values can correspond to strong electrostatic interactions or hydrogen bonding and are not by themselves diagnostic of any specific mechanism. The calculation of $\Delta G°$ from the Langmuir equilibrium constant requires careful attention to the dimensions of the equilibrium constant; the use of dimensional Langmuir constants in $\Delta G° = -RT \ln K_L$ leads to systematically biased thermodynamic parameters, and recent methodological work has proposed corrections to address this issue [98].

6.4. Continuous-Flow Behaviour and Mechanism Validation

Most published AWDB adsorption studies are conducted in batch mode. Practical wastewater and gas-treatment applications, however, operate in continuous-flow configurations such as fixed-bed columns, where breakthrough curves and bed capacity are the relevant performance metrics. The Thomas, Yoon–Nelson, Bohart–Adams and Wolborska models are commonly applied to fit breakthrough data. Real fixed-bed performance is influenced by hydrodynamic factors (channelling, axial dispersion), mass-transfer resistance, competitive adsorption in multicomponent matrices and adsorbent attrition, all of which are absent from idealised plug-flow models [17]. Bridging the gap between batch equilibrium measurements and continuous-flow performance is one of the practical challenges that limits the translation of laboratory AWDB results to industrial deployment. Reliable mechanism identification ultimately requires convergence of evidence from multiple independent techniques: pH-dependent zeta potential, ionic-strength experiments, FTIR and XPS before and after adsorption, competitive adsorption with mechanism-blocking co-solvents, and density-functional-theory (DFT) calculations or molecular-dynamics simulations of solvated adsorbate–surface interactions [24].

7. Critical Perspectives on AWDB Research

The preceding sections summarise the rapidly expanding body of research on AWDB for environmental applications. A critical reading nonetheless reveals several systemic limitations that constrain practical relevance and must be addressed if AWDB is to move from laboratory demonstration to

deployable technology. These limitations are not unique to AWDB but are particularly acute given the diversity of feedstocks, production conditions, and reporting practices in this literature.

7.1. Over-Reliance on Equilibrium Capacity Metrics

The maximum equilibrium adsorption capacity (q_m) derived from Langmuir fits dominates the metrics reported in AWDB studies. While q_m provides a convenient single-number comparison, it has several weaknesses. It is determined under idealised batch conditions that bear little resemblance to operational treatment systems; it is sensitive to the experimental concentration range used in its determination, often extrapolated beyond the tested range, and rarely accompanied by uncertainty estimates; and, most importantly, it provides limited information about kinetic, dynamic, or competitive performance under realistic operating conditions [18,19]. Reporting standards should accordingly include adsorption capacity at environmentally relevant concentrations, complete kinetic profiles, and breakthrough behaviour in fixed-bed configurations alongside the conventional q_m value.

7.2. Inconsistent Testing Conditions and Apparent vs. True Removal

Experimental conditions in AWDB studies vary widely. Initial pollutant concentrations span four to five orders of magnitude, adsorbent doses range from sub-g·L^{-1} to tens of g·L^{-1}, and pH values cover the full range from strongly acidic to strongly alkaline, often without justification linked to the target wastewater matrix. The result is that nominally comparable studies on similar feedstocks frequently produce vastly different performance metrics. Convergence on a small set of standardised testing protocols, analogous to those used in commercial activated-carbon evaluation would substantially improve the value of the published literature. A related concern is the distinction between true sorption and concurrent removal mechanisms. Metal-hydroxide precipitation at near-neutral or alkaline pH can yield removal efficiencies above 90% in the absence of any specific adsorbent activity; the alkaline character of many high-temperature biochars raises solution pH on contact, potentially shifting metal speciation toward precipitating forms [99]. Without careful pH control, speciation analysis, and blank experiments, removal efficiencies can be substantially overestimated.

7.3. Limited Multicomponent Studies and Mechanistic Validation

Real wastewaters, contaminated soils, and industrial gas streams are complex matrices containing multiple competing adsorbates, dissolved organic matter, suspended solids, and a range of inorganic ions. Single-solute laboratory experiments with deionised water systematically overestimate performance relative to real conditions. Multicomponent studies—for example, the simultaneous adsorption of several heavy metals, or of antibiotics in the presence of humic acid—generally report lower capacities than the corresponding single-solute experiments; competitive sorption of norfloxacin, sulfamerazine, and oxytetracycline on KOH-modified biochar, for instance, differs from the corresponding single-solute systems in both kinetics and equilibrium distribution [79]. The magnitude of the reduction is system-specific, and no representative range can responsibly be quoted from the current literature, because competitive data exist for only a small and non-random subset of adsorbate combinations. Mechanistic claims in the AWDB literature are also frequently based on isotherm and kinetic-model fits alone, sometimes supplemented by FTIR peak-shift observations of variable rigour. Independent confirmation through XPS, zeta-potential analysis, competitive-adsorption experiments, or computational modelling remains comparatively rare. Claims of "chemisorption" inferred solely from PSO kinetic fits, or of "π–π stacking" inferred solely from the presence of aromatic adsorbates, fall short of rigorous mechanistic identification.

7.4. Regeneration, Stability, and Life-Cycle Considerations

Practical adsorbent operation requires multiple cycles of adsorption and regeneration. AWDB regeneration typically uses acidic, basic, or organic-solvent washes whose environmental and economic costs are seldom reported. Repeated cycles can degrade surface functional groups, reduce surface area through pore collapse, and generate secondary waste streams that require further management. Reports of "high reusability" based on three to five cycles in batch experiments under near-ideal conditions do not necessarily extrapolate to industrial cycle counts of hundreds to thousands [18,95]. Equally important is the broader environmental footprint of the adsorbent: the energy demand of high-temperature pyrolysis, the chemical waste from KOH or $ZnCl_2$ activation, and the transport burden of biomass collection and biochar distribution all contribute to the cradle-to-grave impact of AWDB. Comprehensive life-cycle assessments remain scarce, although those published indicate that the net carbon balance of AWDB is generally favourable but strongly dependent on system boundaries and reference baselines [54,93]. Techno-economic analyses similarly indicate that AWDB can be cost-competitive with commercial activated carbon under favourable conditions (cheap biomass, integrated heat recovery, productive end use), but is not universally so [38].

7.5. Safety, Contaminant Leaching, and End-of-Life Management

Assessments of AWDB rarely extend to the risks created by the material itself. Pyrolysis generates polycyclic aromatic hydrocarbons (PAHs) and other condensable organics that can remain sorbed on the char, in amounts that depend strongly on reactor design, vapour residence time, heating rate, and post-treatment. Slow pyrolysis with efficient vapour removal generally yields low PAH loads, whereas poorly ventilated or low-temperature conditions can produce material that exceeds the thresholds set by biochar certification schemes [91,92]. Reported total PAH contents in biochars span more than two orders of magnitude, and the bioavailable fraction is generally a small but variable proportion of the total, so that total-content measurements alone are a conservative rather than a precise indicator of risk. Routine reporting of PAH content, together with the extraction method used to determine it, is a reasonable minimum requirement for any biochar proposed for soil application [51,52].

Inorganic contaminants deserve equal attention. Because the mineral fraction of the feedstock is concentrated in the solid product, potentially toxic elements already present in the residue are enriched in the biochar; Cd and As in rice straw and husk grown on contaminated soils are the clearest example, and these are precisely the feedstocks most abundant in the regions where AWDB deployment is most often proposed. Chloride and alkali salts in some cereal residues create a salinity risk at high application rates. Composite and impregnated biochars introduce a further pathway: Fe, Mn, Ni, Zn, or Cu introduced deliberately during modification can be released in acidic or complexing media, yet leaching of the impregnated phase is seldom quantified across the pH range relevant to the intended application. For magnetic and metal-oxide composites in particular, metal-release testing under realistic conditions should accompany any claim of adsorption performance.

End-of-life management of spent adsorbent is the least developed part of the AWDB literature. Biochar loaded with heavy metals, dyes or antibiotics is a concentrated waste stream, and its fate is rarely addressed beyond a statement that the material can be regenerated. The realistic options—thermal reactivation, chemical desorption with recovery of the desorbate, stabilisation and disposal as hazardous waste, or, for organic loadings only, destruction by incineration—differ substantially in cost and environmental burden, and the choice among them determines whether the low-cost framing of AWDB survives a full accounting. The wash-waters generated by KOH, $ZnCl_2$ or H_3PO_4 activation present a parallel problem: neutralisation, zinc or phosphate recovery, and effluent treatment carry costs and impacts that are almost never included in the comparisons drawn with commercial activated carbon. Life-cycle assessments of AWDB should

therefore bring activation-agent production and recovery, spent-adsorbent disposal, and any contaminant-release burden within their system boundaries.

8. Future Research Directions

The limitations identified in Section 7 point to a set of priorities for the next generation of AWDB studies. Several have been articulated in earlier reviews; their adoption by the broader research community remains incomplete.

First, future studies should converge on standard protocols for batch and continuous-flow performance evaluation, with environmentally relevant pollutant concentrations, realistic adsorbent doses, controlled pH and ionic strength conditions representative of real water matrices, and the reporting of complete kinetic profiles rather than only equilibrium values. Inter-laboratory ring trials would help to validate performance claims and to identify methodological inconsistencies. Second, the dominant pattern of empirical screening across feedstocks and activation conditions, followed by post-hoc rationalisation, should give way to mechanism-guided design: the target pollutant, application context, and required interaction modes should be specified first, with the precursor, carbonisation conditions, activation route, and surface modification then chosen to deliver the required combination of pore structure and surface chemistry [24]. Third, performance testing in single-solute synthetic solutions should give way to studies in realistic multicomponent matrices and, where possible, in actual industrial wastewaters; pilot-scale studies in real treatment plants, while costly, are essential for genuine performance validation.

Fourth, the growing volume of published AWDB data on production conditions, structural properties, and performance metrics presents an opportunity for data-driven material design through machine-learning approaches. Curated databases linking precursor, processing conditions, and performance can train predictive models that suggest optimal synthesis parameters for given application targets. Recent demonstrations of machine-learning-based prediction of CO_2 adsorption on KOH-activated biochar [60,100] and of hybrid optimisation frameworks that couple machine learning with experimental screening for the design of antibiotic-removal biochars [101] illustrate the promise. The success of such efforts depends critically on the quality and consistency of the underlying experimental data, reinforcing the need for standardised reporting. Fifth, comprehensive cradle-to-grave life-cycle assessments and techno-economic analyses should accompany any claim of practical viability for AWDB. System boundaries should encompass feedstock collection and transport, energy inputs for carbonisation and activation, chemical inputs and waste streams from activation, water and energy inputs for regeneration, and the final disposal or beneficial reuse of spent adsorbent. Comparisons with commercial activated carbon should be made on a like-for-like basis under realistic operating conditions rather than on a unit-mass basis at idealised laboratory performance [54,93]. Reported model performance should be interpreted in the light of the heterogeneity of the training data: models trained on literature compilations inherit the reporting inconsistencies described in Section 7.2, and external validation on independently generated data is rarely presented.

Sixth, reducing the environmental and economic burden of biochar production is a central practical challenge. Promising directions include low-energy carbonisation via microwave-assisted or solar pyrolysis, reduced reliance on corrosive activating agents through alternative chemistries (such as K_2CO_3, $NaHCO_3$ or biopolymer-based activators), and integration of biochar production with anaerobic digestion or other waste-treatment processes to share infrastructure and reduce specific energy requirements. Seventh, single-function biochar materials are increasingly being supplanted by multifunctional composites that combine adsorption with magnetic recovery, catalysis, redox activity, or controlled-release functionality. Future research should examine the synergistic effects of such combinations and address the additional complexity they introduce in production cost, regeneration, and end-of-life management. Finally, beyond technical research, the practical deployment of AWDB depends on regulatory frameworks that recognise biochar as a legitimate soil amendment and waste-management technology and that provide market signals for the

carbon-sequestration value of stable biochar carbon. The integration of biochar into national and international carbon-accounting protocols is an active area of policy development [93] and requires sustained engagement among the research community, industry, and policymakers. Eighth, safety and end-of-life management should be brought into the standard reporting set for AWDB studies, as set out in Section 7.5: residual pyrolysis organics and potentially toxic elements should be measured against established certification thresholds [51,52], release of impregnated metals should be quantified over the relevant pH range, and the disposal or reactivation route for pollutant-loaded spent adsorbent should be identified and costed rather than left implicit.

9. Conclusions

Agricultural waste–derived biochar has emerged as a versatile, multifunctional class of carbonaceous adsorbent with significant promise for environmental remediation and circular waste management. The combination of abundant feedstocks available at low or negative gate cost, tunable physicochemical properties, and a broad application envelope spanning water treatment, soil amendment, and carbon sequestration accounts for the rapid expansion of research in this area over the past decade. That low-cost framing applies to the raw residue rather than to the delivered adsorbent: collection, drying, storage, and transport, and for activated materials, the production and recovery of the activating agent together with treatment of the resulting wash-waters, are rarely brought inside the comparison. This review has examined the production, activation, characterisation and environmental applications of AWDB with emphasis on developments published between 2020 and 2026. Several conclusions emerge. The performance of AWDB is governed by a synthesis–structure–function relationship in which feedstock composition, carbonisation pathway, activation strategy, and surface modification jointly determine pore architecture and surface chemistry; optimal performance requires alignment of these properties with the physicochemical characteristics of the target pollutant rather than maximisation of surface area alone. Application-specific design principles have become clearer: ultramicroporous, nitrogen-doped biochars are preferred for CO_2 capture; mesoporous, oxygen-rich biochars for dye and pharmaceutical adsorption; and functional-group-rich biochars for heavy-metal removal. The field nonetheless remains constrained by methodological limitations—over-reliance on equilibrium-capacity metrics, inconsistent testing conditions, limited multicomponent studies, and inadequate mechanistic validation—that hinder the translation of laboratory results into deployable technology. These conclusions rest on an evidence base whose composition is documented in Section 1.1, and several of them are conditional rather than general: the energy advantage claimed for microwave-assisted pyrolysis, the economic comparison between hydrothermal carbonisation and pyrolysis, the magnitude of field crop-yield response and the centennial stability of biochar carbon are each sensitive to feedstock, system boundary, operating conditions and evidence quality, and are stated here as such. Comparisons of surface area and CO_2 uptake with commercial activated carbons are meaningful only when the distinction between biochar, activated biochar, and biochar-derived activated carbon is preserved.

Future research priorities include standardisation of performance testing, mechanism-guided rather than empirical synthesis, multicomponent and matrix-effect studies, data-driven material design, comprehensive life-cycle and techno-economic assessment, scalable green synthesis routes, multifunctional composite systems, and rigorous soil-application evaluation. Achieving these priorities will require sustained, multidisciplinary effort that connects materials chemistry, environmental engineering, soil science, and policy. The continued maturation of AWDB research, together with parallel developments in adjacent classes of biomass-derived carbon materials, indicates a credible but as yet unproven route toward deployment, and each of the attributes commonly claimed for AWDB is conditional rather than established. Scalability is constrained by the seasonality and spatial dispersion of residue supply, by feedstock heterogeneity that propagates into product variability, and by the small number of reactor configurations demonstrated beyond pilot scale. Economic viability is site- and boundary-specific: the advantage over

commercial activated carbon narrows, and in some accounts disappears, once collection and transport, activating-agent production and recovery, wash-water treatment, and spent-adsorbent disposal are brought inside the system boundary. Environmental benefit is contingent on the energy source used for carbonisation, on the management of pyrolysis gases and liquids, and on the PAH, potentially toxic element and ash burden carried by the product, none of which is consistently reported. Field responses in soil application are considerably more variable than pot-trial responses and include neutral and negative outcomes, particularly on fertile temperate soils and where over-alkalinisation or salinity risk is present. On the present evidence, AWDB is therefore most accurately described as a promising material class with demonstrated laboratory efficacy and unresolved deployment economics, rather than as an established low-cost and sustainable technology; establishing the latter will require life-cycle and techno-economic assessment with transparent and comparable system boundaries, long-term field trials across contrasting soils and climates, and explicit end-of-life management strategies. The transition from a promising research material to a deployable technology will depend not on incremental improvements in single-pollutant performance metrics but on a systemic shift toward mechanism-guided design, standardised evaluation, and integration with broader circular-economy and climate-mitigation frameworks. A further requirement, largely absent from the present literature, is that the safety profile of the material—residual pyrolysis organics, potentially toxic elements inherited from the feedstock, release of deliberately impregnated metals, and the disposal or reactivation of pollutant-loaded spent adsorbent—be reported alongside its performance rather than assumed to be benign.

Statement of the Use of Generative AI and AI-Assisted Technologies in the Writing Process

During the preparation of this work the authors used generative artificial-intelligence writing assistants based on large language models in order to improve the readability and language of selected sections of the text. No artificial-intelligence tool was used to define the scope of the review, to conduct the literature search or screening, to extract, analyse or interpret data, to generate the figures or tables, or to formulate the scientific conclusions. After using these tools the authors reviewed and edited the content as required and take full responsibility for the content of the published article.

Acknowledgments

The authors are grateful to Swaminarayan University for institutional support, laboratory facilities and the academic environment in which this review was prepared. The authors thank the broader biochar research community whose published work made this synthesis possible.

Author Contributions

Conceptualization, H.V.V. and K.G.P.; Investigation, H.V.V., P.J.P. and P.V.; Writing—Original Draft Preparation, H.V.V. and P.J.P.; Writing—Review & Editing, P.V. and K.G.P.; Visualization, P.J.P.; Supervision, K.G.P. All authors have read and agreed to the published version of the manuscript.

Ethics Statement

Not applicable. This work is a review article that does not involve studies with human participants or animals performed by any of the authors.

Informed Consent Statement

Not applicable.

Data Availability Statement

No new primary data were generated for this review. Numerical values reproduced in the article are attributed to the cited literature and are reported as given in the original sources. As a structured narrative review, this article does not present a pooled or systematically screened dataset.

Funding

This research received no external funding.

Declaration of Competing Interest

The authors declare that they have no known competing financial interests or personal relationships that could have appeared to influence the work reported in this paper.

References

1. Lal R. World crop residues production and implications of its use as a biofuel. *Environ. Int.* **2005**, *31*, 575–584. DOI:10.1016/j.envint.2004.09.005
2. Tripathi N, Hills CD, Singh RS, Atkinson CJ. Biomass waste utilisation in low-carbon products. *npj Clim. Atmos. Sci.* **2019**, *2*, 35. DOI:10.1038/s41612-019-0093-5
3. Bhuvaneshwari S, Hettiarachchi H, Meegoda JN. Crop Residue Burning in India: Policy Challenges and Potential Solutions. *Int. J. Environ. Res. Public Health* **2019**, *16*, 832. DOI:10.3390/ijerph16050832
4. Jain N, Bhatia A, Pathak H. Emission of Air Pollutants from Crop Residue Burning in India. *Aerosol Air Qual. Res.* **2014**, *14*, 422–430. DOI:10.4209/aaqr.2013.01.0031
5. Lehmann J, Joseph S. (Eds.). *Biochar for Environmental Management: Science, Technology and Implementation*, 2nd ed.; Routledge: London, UK, 2015.
6. Sohi SP, Krull E, Lopez-Capel E, Bol R. A Review of Biochar and Its Use and Function in Soil. *Adv. Agron.* **2010**, *105*, 47–82. DOI:10.1016/S0065-2113(10)05002-9
7. Tan X, Liu Y, Zeng G, Wang X, Hu X, Gu Y, et al. Application of biochar for the removal of pollutants from aqueous solutions. *Chemosphere* **2015**, *125*, 70–85. DOI:10.1016/j.chemosphere.2014.12.058
8. Ahmad M, Rajapaksha AU, Lim JE, Zhang M, Bolan N, Mohan D, et al. Biochar as a sorbent for contaminant management in soil and water. *Chemosphere* **2014**, *99*, 19–33. DOI:10.1016/j.chemosphere.2013.10.071
9. Wang J, Wang S. Preparation, modification and environmental application of biochar: A review. *J. Clean. Prod.* **2019**, *227*, 1002–1022. DOI:10.1016/j.jclepro.2019.04.282
10. Wu P, Fu Y, Vancov T, Wang H, Wang Y, Chen W. Analyzing the trends and hotspots of biochar's applications in agriculture, environment, and energy: a bibliometrics study for 2022 and 2023. *Biochar* **2024**, *6*, 78. DOI:10.1007/s42773-024-00370-x
11. Wang T, Zhai Y, Zhu Y, Li C, Zeng G. A review of the hydrothermal carbonization of biomass waste for hydrochar formation: Process conditions, fundamentals, and physicochemical properties. *Renew. Sustain. Energy Rev.* **2018**, *90*, 223–247. DOI:10.1016/j.rser.2018.03.071
12. Foong SY, Liew RK, Yang Y, Cheng YW, Yek PNY, Wan Mahari WA, et al. Valorization of biomass waste to engineered activated biochar by microwave pyrolysis. *Chem. Eng. J.* **2020**, *389*, 124401. DOI:10.1016/j.cej.2020.124401
13. Marsh H, Rodríguez-Reinoso F. *Activated Carbon*; Elsevier: Amsterdam, The Netherlands, 2006.
14. Sevilla M, Díez N, Fuertes AB. More Sustainable Chemical Activation Strategies for the Production of Porous Carbons. *ChemSusChem* **2021**, *14*, 94–117. DOI:10.1002/cssc.202001838
15. Ashiq A, Adassooriya NM, Sarkar B, Rajapaksha AU, Ok YS, Vithanage M. Municipal solid waste biochar-bentonite composite for the removal of antibiotic ciprofloxacin from aqueous media. *J. Environ. Manag.* **2019**, *236*, 428–435. DOI:10.1016/j.jenvman.2019.02.006
16. Latifian B, Taghizade Firozjaee T, Abdi J. Synthesis of biochar-iron oxide magnetic nanocomposite for efficient and rapid removal of Pb(II) heavy metal from water. *Water Pract. Technol.* **2024**, *19*, 181–199. DOI:10.2166/wpt.2023.223
17. Patel H. Fixed-bed column adsorption study: A comprehensive review. *Appl. Water Sci.* **2019**, *9*, 45. DOI:10.1007/s13201-019-0927-7
18. Tran HN, You SJ, Hosseini-Bandegharaei A, Chao HP. Mistakes and inconsistencies regarding adsorption of contaminants from aqueous solutions: A critical review. *Water Res.* **2017**, *120*, 88–116. DOI:10.1016/j.watres.2017.04.014

19. Tran HN. Comments on "High-efficiency removal of dyes from wastewater by fully recycling litchi peel biochar". *Chemosphere* **2020**, *257*, 126444. DOI:10.1016/j.chemosphere.2020.126444
20. Page MJ, McKenzie JE, Bossuyt PM, Boutron I, Hoffmann TC, Mulrow CD, et al. The PRISMA 2020 statement: An updated guideline for reporting systematic reviews. *BMJ* **2021**, *372*, n71. DOI:10.1136/bmj.n71
21. Patel MR, Panwar NL. Biochar from agricultural crop residues: Environmental, production, and life cycle assessment overview. *Resour. Conserv. Recycl. Adv.* **2023**, *19*, 200173. DOI:10.1016/j.rcradv.2023.200173
22. Inyang MI, Gao B, Yao Y, Xue Y, Zimmerman A, Mosa A, et al. A review of biochar as a low-cost adsorbent for aqueous heavy metal removal. *Crit. Rev. Environ. Sci. Technol.* **2016**, *46*, 406–433. DOI:10.1080/10643389.2015.1096880
23. Hama Aziz KH, Fatah NM, Muhammad KT. Advancements in application of modified biochar as a green and low-cost adsorbent for wastewater remediation from organic dyes. *R. Soc. Open Sci.* **2024**, *11*, 232033. DOI:10.1098/rsos.232033
24. Liu Z, Xu Z, Xu L, Buyong F, Chay TC, Li Z, et al. Modified biochar: Synthesis and mechanism for removal of environmental heavy metals. *Carbon Res.* **2022**, *1*, 100096. DOI:10.1007/s44246-022-00007-3
25. Mohan D, Sarswat A, Ok YS, Pittman CU. Organic and inorganic contaminants removal from water with biochar. *Bioresour. Technol.* **2014**, *160*, 191–202. DOI:10.1016/j.biortech.2014.01.120
26. Yang H, Yan R, Chen H, Lee DH, Zheng C. Characteristics of hemicellulose, cellulose and lignin pyrolysis. *Fuel* **2007**, *86*, 1781–1788. DOI:10.1016/j.fuel.2006.12.013
27. Keiluweit M, Nico PS, Johnson MG, Kleber M. Dynamic Molecular Structure of Plant Biomass-Derived Black Carbon (Biochar). *Environ. Sci. Technol.* **2010**, *44*, 1247–1253. DOI:10.1021/es9031419
28. Zhu W, Chen F, Ye L, Yang X, Song Y, Wang H. Methylene blue and acid red adsorption on biochar made from modified sugarcane bagasse. *Adsorpt. Sci. Technol.* **2024**, *42*, 02636174241273522. DOI:10.1177/02636174241273522
29. Cha JS, Park SH, Jung SC, Ryu C, Jeon JK, Shin MC, et al. Production and utilization of biochar: A review. *J. Ind. Eng. Chem.* **2016**, *40*, 1–15. DOI:10.1016/j.jiec.2016.06.002
30. Demirbas A. Effects of temperature and particle size on bio-char yield from pyrolysis of agricultural residues. *J. Anal. Appl. Pyrolysis* **2004**, *72*, 243–248. DOI:10.1016/j.jaap.2004.07.003
31. Ronsse F, van Hecke S, Dickinson D, Prins W. Production and characterization of slow pyrolysis biochar: Influence of feedstock type and pyrolysis conditions. *GCB Bioenergy* **2013**, *5*, 104–115. DOI:10.1111/gcbb.12018
32. Li Z, Su Q, Xiang L, Yuan Y, Tu S. Effect of Pyrolysis Temperature on the Sorption of Cd(II) and Se(IV) by Rice Husk Biochar. *Plants* **2022**, *11*, 3234. DOI:10.3390/plants11233234
33. Khater ES, Bahnasawy A, Hamouda R, Sabahy A, Abbas W, Morsy OM. Biochar production under different pyrolysis temperatures with different types of agricultural wastes. *Sci. Rep.* **2024**, *14*, 36812. DOI:10.1038/s41598-024-52336-5
34. Bridgwater AV. Review of fast pyrolysis of biomass and product upgrading. *Biomass Bioenergy* **2012**, *38*, 68–94. DOI:10.1016/j.biombioe.2011.01.048
35. Kuo LA, Tsai WT, Yang RY, Tsai JH. Production of High-Porosity Biochar from Rice Husk by the Microwave Pyrolysis Process. *Processes* **2023**, *11*, 3119. DOI:10.3390/pr11113119
36. Funke A, Ziegler F. Hydrothermal carbonization of biomass: A summary and discussion of chemical mechanisms for process engineering. *Biofuels Bioprod Bioref* **2010**, *4*, 160–177. DOI:10.1002/bbb.198
37. Petrović J, Ercegović M, Simić M, Koprivica M, Dimitrijević J, Jovanović A, et al. Hydrothermal Carbonization of Waste Biomass: A Review of Hydrochar Preparation and Environmental Application. *Processes* **2024**, *12*, 207. DOI:10.3390/pr12010207
38. Gamaralalage D, Rodgers S, Gill A, Meredith W, Bott T, West H, et al. Biowaste to biochar: A techno-economic and life cycle assessment of biochar production from food-waste digestate and its agricultural field application. *Biochar* **2025**, *7*, 50. DOI:10.1007/s42773-025-00456-0
39. Huang Z, Wang Q, Zhang Y, Du B, Zhou J, Ji D. Effects of Pyrolysis Temperatures and Modified Methods on Rice Husk-Derived Biochar Characteristics and Heavy Metal Adsorption. *Molecules* **2025**, *30*, 3616. DOI:10.3390/molecules30173616
40. Li D, Ma T, Zhang R, Tian Y, Qiao Y. Preparation of porous carbons with high low-pressure CO_2 uptake by KOH activation of rice husk char. *Fuel* **2015**, *139*, 68–70. DOI:10.1016/j.fuel.2014.08.027
41. Presser V, McDonough J, Yeon SH, Gogotsi Y. Effect of pore size on carbon dioxide sorption by carbide derived carbon. *Energy Environ. Sci.* **2011**, *4*, 3059. DOI:10.1039/c1ee01176f
42. Lillo-Ródenas MA, Cazorla-Amorós D, Linares-Solano A. Understanding chemical reactions between carbons and NaOH and KOH. *Carbon* **2003**, *41*, 267–275. DOI:10.1016/S0008-6223(02)00279-8
43. Hassan MM, Carr CM. Biomass-derived porous carbonaceous materials and their composites as adsorbents for cationic and anionic dyes: A review. *Chemosphere* **2021**, *265*, 129087. DOI:10.1016/j.chemosphere.2020.129087

44. Li J, Michalkiewicz B, Min J, Ma C, Chen X, Gong J, et al. Selective preparation of biomass-derived porous carbon with controllable pore sizes toward highly efficient CO_2 capture. *Chem. Eng. J.* **2019**, *360*, 250–259. DOI:10.1016/j.cej.2018.11.204
45. Singh MG, Lakhi KS, Park D, Srivastava P, Naidu R, Vinu A. Facile One-Pot Synthesis of Activated Porous Biocarbons with a High Nitrogen Content for CO_2 Capture. *ChemNanoMat* **2018**, *4*, 281–290. DOI:10.1002/cnma.201700348
46. Sun Y, Jia J, Liu Z, Liu Z, Huo L, Zhao L, et al. Heteroatom-doped biochar devised from cellulose for CO_2 adsorption. *Biochar* **2023**, *5*, 76. DOI:10.1007/s42773-023-00275-1
47. Janu R, Mrlik V, Ribitsch D, Hofman J, Sedláček P, Bielská L, et al. Biochar surface functional groups as affected by biomass feedstock, biochar composition and pyrolysis temperature. *Carbon Resour. Convers.* **2021**, *4*, 36–46. DOI:10.1016/j.crcon.2021.01.003
48. Yang X, Wan Y, Zheng Y, He F, Yu Z, Huang J, et al. Surface functional groups of carbon-based adsorbents and their roles in the removal of heavy metals from aqueous solutions: A critical review. *Chem. Eng. J.* **2019**, *366*, 608–621. DOI:10.1016/j.cej.2019.02.119
49. Aziz S, Anbreen S, Iftikhar I, Fatima T, Iftikhar A, Ali L. Green technology: synthesis of iron-modified biochar derived from pine cones to remove azithromycin and ciprofloxacin from water. *Front. Environ. Sci.* **2024**, *12*, 1353267. DOI:10.3389/fenvs.2024.1353267
50. Geetha T, Smitha JK, Sebastian M, Litty MI, Joseph B, Joseph J, et al. Synthesis and characterization of nano iron oxide biochar composite for efficient removal of crystal violet from water. *Heliyon* **2024**, *10*, e39450. DOI:10.1016/j.heliyon.2024.e39450
51. European Biochar Certificate (EBC). *Guidelines for a Sustainable Production of Biochar, Version 10.3*; Carbon Standards International: Frick, Switzerland, 2023.
52. International Biochar Initiative (IBI). *Standardized Product Definition and Product Testing Guidelines for Biochar That Is Used in Soil, Version 2.1*; International Biochar Initiative: Canandaigua, NY, USA, 2015.
53. Aller D, Bakshi S, Laird DA. Modified method for proximate analysis of biochars. *J. Anal. Appl. Pyrolysis* **2017**, *124*, 335–342. DOI:10.1016/j.jaap.2017.01.012
54. Wang J, Xiong Z, Kuzyakov Y. Biochar stability in soil: Meta-analysis of decomposition and priming effects. *GCB Bioenergy* **2016**, *8*, 512–523. DOI:10.1111/gcbb.12266
55. Spokas KA. Review of the stability of biochar in soils: Predictability of O:C molar ratios. *Carbon Manag.* **2010**, *1*, 289–303. DOI:10.4155/cmt.10.32
56. Brunauer S, Emmett PH, Teller E. Adsorption of Gases in Multimolecular Layers. *J. Am. Chem. Soc.* **1938**, *60*, 309–319. DOI:10.1021/ja01269a023
57. Lozano-Castelló D, Cazorla-Amorós D, Linares-Solano A. Usefulness of CO_2 adsorption at 273 K for the characterization of porous carbons. *Carbon* **2004**, *42*, 1233–1242. DOI:10.1016/j.carbon.2004.01.037
58. Ferrari AC, Robertson J. Interpretation of Raman spectra of disordered and amorphous carbon. *Phys. Rev. B* **2000**, *61*, 14095–14107. DOI:10.1103/PhysRevB.61.14095
59. Amen R, Yaseen M, Mukhtar A, Klemeš JJ, Saqib S, Ullah S, et al. Lead and cadmium removal from wastewater using eco-friendly biochar adsorbent derived from rice husk, wheat straw, and corncob. *Clean. Eng. Technol.* **2020**, *1*, 100006. DOI:10.1016/j.clet.2020.100006
60. Hassan R, Baghban A. Predicting CO_2 adsorption in KOH-activated biochar using advanced machine learning techniques. *Sci. Rep.* **2025**, *15*, 24410. DOI:10.1038/s41598-025-09248-9
61. Hassan M, Liu Y, Naidu R, Parikh SJ, Du J, Qi F, et al. Influences of feedstock sources and pyrolysis temperature on the properties of biochar and functionality as adsorbents: A meta-analysis. *Sci. Total Environ.* **2020**, *744*, 140714. DOI:10.1016/j.scitotenv.2020.140714
62. Cui X, Hao H, Zhang C, He Z, Yang X. Capacity and mechanisms of ammonium and cadmium sorption on different wetland-plant derived biochars. *Sci. Total Environ.* **2016**, *539*, 566–575. DOI:10.1016/j.scitotenv.2015.09.022
63. Li H, Dong X, da Silva EB, de Oliveira LM, Chen Y, Ma LQ. Mechanisms of metal sorption by biochars: Biochar characteristics and modifications. *Chemosphere* **2017**, *178*, 466–478. DOI:10.1016/j.chemosphere.2017.03.072
64. Park JH, Choppala G, Lee SJ, Bolan N, Chung JW, Edraki M. Comparative Sorption of Pb and Cd by Biochars and Its Implication for Metal Immobilization in Soils. *Water Air Soil Pollut.* **2013**, *224*, 1711. DOI:10.1007/s11270-013-1711-1
65. Đukanović N, Apostolović T, Anojčić J, Mutić S, Marjanović Srebro T, Kozma G, et al. Comparative Study of Biochar from Different Biomass Feedstocks: Toward Sustainable Resource Utilization and Environmental Applications. *Molecules* **2026**, *31*, 37. DOI:10.3390/molecules31010037

66. Bashir S, Hussain Q, Akmal M, Riaz M, Hu H, Ijaz SS, et al. Sugarcane bagasse-derived biochar reduces the cadmium and chromium bioavailability to mash bean and enhances the microbial activity in contaminated soil. *J. Soils Sediments* **2018**, *18*, 874–886. DOI:10.1007/s11368-017-1796-z
67. Naeem MA, Khalid M, Aon M, Abbas G, Tahir M, Amjad M, et al. Effect of wheat and rice straw biochar produced at different temperatures on maize growth and nutrient dynamics of a calcareous soil. *Arch. Agron. Soil Sci.* **2017**, *63*, 2048–2061. DOI:10.1080/03650340.2017.1325468
68. Gholami L, Rahimi G, Khademi Jolgeh Nezhad A. Effect of thiourea-modified biochar on adsorption and fractionation of cadmium and lead in contaminated acidic soil. *Int. J. Phytoremediation* **2020**, *22*, 468–481. DOI:10.1080/15226514.2019.1678108
69. Beesley L, Moreno-Jiménez E, Gomez-Eyles JL, Harris E, Robinson B, Sizmur T. A review of biochars' potential role in the remediation, revegetation and restoration of contaminated soils. *Environ. Pollut.* **2011**, *159*, 3269–3282. DOI:10.1016/j.envpol.2011.07.023
70. Jeffery S, Verheijen FGA, van der Velde M, Bastos AC. A quantitative review of the effects of biochar application to soils on crop productivity using meta-analysis. *Agric. Ecosyst. Environ.* **2011**, *144*, 175–187. DOI:10.1016/j.agee.2011.08.015
71. Jeffery S, Abalos D, Prodana M, Bastos AC, van Groenigen JW, Hungate BA, et al. Biochar boosts tropical but not temperate crop yields. *Environ. Res. Lett.* **2017**, *12*, 053001. DOI:10.1088/1748-9326/aa67bd
72. Tkaczyk A, Mitrowska K, Posyniak A. Synthetic organic dyes as contaminants of the aquatic environment and their implications for ecosystems: A review. *Sci. Total Environ.* **2020**, *717*, 137222. DOI:10.1016/j.scitotenv.2020.137222
73. Michael I, Rizzo L, McArdell CS, Manaia CM, Merlin C, Schwartz T, et al. Urban wastewater treatment plants as hotspots for the release of antibiotics in the environment: A review. *Water Res.* **2013**, *47*, 957–995. DOI:10.1016/j.watres.2012.11.027
74. Ahmed MB, Zhou JL, Ngo HH, Guo W. Adsorptive removal of antibiotics from water and wastewater: Progress and challenges. *Sci. Total Environ.* **2015**, *532*, 112–126. DOI:10.1016/j.scitotenv.2015.05.130
75. Patel M, Kumar R, Kishor K, Mlsna T, Pittman CU, Mohan D. Pharmaceuticals of Emerging Concern in Aquatic Systems: Chemistry, Occurrence, Effects, and Removal Methods. *Chem. Rev.* **2019**, *119*, 3510–3673. DOI:10.1021/acs.chemrev.8b00299
76. Yao J, Ji J, Zhang J, Fang J. Molecular structure-dependent adsorption mechanisms of tetracycline antibiotics congeners on biochar. *Biochar X* **2026**, *2*, e008. DOI:10.48130/bchax-0026-0007
77. Zeng Z, Tan X, Liu Y, Tian S, Zeng G, Jiang L, et al. Comprehensive Adsorption Studies of Doxycycline and Ciprofloxacin Antibiotics by Biochars Prepared at Different Temperatures. *Front. Chem.* **2018**, *6*, 80. DOI:10.3389/fchem.2018.00080
78. Liu Y, Gao W, Yin S, Liu R, Li Z. Efficient removal of tetracycline from aqueous solution by K_2CO_3 activated penicillin fermentation residue biochar. *Front. Chem.* **2022**, *10*, 1078877. DOI:10.3389/fchem.2022.1078877
79. Luo J, Li X, Ge C, Müller K, Yu H, Huang P, et al. Sorption of norfloxacin, sulfamerazine and oxytetracycline by KOH-modified biochar under single and ternary systems. *Bioresour. Technol.* **2018**, *263*, 385–392. DOI:10.1016/j.biortech.2018.05.022
80. Liang H, Zhu C, Wang A, Chen F. Facile preparation of $NiFe_2O_4$/biochar composite adsorbent for efficient adsorption removal of antibiotics in water. *Carbon Res.* **2024**, *3*, 2. DOI:10.1007/s44246-023-00094-w
81. Deng Y, Xiao T, She A, Li X, Chen W, Ao T, et al. One-step synthesis of iron and nitrogen co-doped porous biochar for efficient removal of tetracycline from water: Adsorption performance and fixed-bed column. *J. Environ. Manag.* **2024**, *352*, 119984. DOI:10.1016/j.jenvman.2023.119984
82. Soo XYD, Lee JJC, Wu WY, Tao L, Wang C, Zhu Q, et al. Advancements in CO_2 capture by absorption and adsorption: A comprehensive review. *J. CO_2 Util.* **2024**, *81*, 102727. DOI:10.1016/j.jcou.2024.102727
83. Plaza MG, González AS, Pevida C, Pis JJ, Rubiera F. Valorisation of spent coffee grounds as CO_2 adsorbents for postcombustion capture applications. *Appl. Energy* **2012**, *99*, 272–279. DOI:10.1016/j.apenergy.2012.05.028
84. Pal A, Uddin K, Saha BB, Thu K, Kil HS, Yoon SH, et al. A benchmark for CO_2 uptake onto newly synthesized biomass-derived activated carbons. *Appl. Energy* **2020**, *264*, 114720. DOI:10.1016/j.apenergy.2020.114720
85. Singh G, Lakhi KS, Sil S, Bhosale SV, Kim I, Albahily K, et al. Biomass derived porous carbon for CO_2 capture. *Carbon* **2019**, *148*, 164–186. DOI:10.1016/j.carbon.2019.03.050
86. Shafawi AN, Mohamed AR, Lahijani P, Mohammadi M. Recent advances in developing engineered biochar for CO_2 capture: An insight into the biochar modification approaches. *J. Environ. Chem. Eng.* **2021**, *9*, 106869. DOI:10.1016/j.jece.2021.106869
87. Glaser B, Lehmann J, Zech W. Ameliorating physical and chemical properties of highly weathered soils in the tropics with charcoal. *Biol. Fertil. Soils* **2002**, *35*, 219–230. DOI:10.1007/s00374-002-0466-4

88. Anyebe O, Sadiq FK, Manono BO, Matsika TA. Biochar Characteristics and Application: Effects on Soil Ecosystem Services and Nutrient Dynamics for Enhanced Crop Yields. *Nitrogen* **2025**, *6*, 31. DOI:10.3390/nitrogen6020031
89. Bo X, Zhang Z, Wang J, Guo S, Li Z, Lin H, et al. Benefits and limitations of biochar for climate-smart agriculture: A review and case study from China. *Biochar* **2023**, *5*, 77. DOI:10.1007/s42773-023-00279-x
90. Hagemann N, Joseph S, Schmidt HP, Kammann CI, Harter J, Borch T, et al. Organic coating on biochar explains its nutrient retention and stimulation of soil fertility. *Nat. Commun.* **2017**, *8*, 1089. DOI:10.1038/s41467-017-01123-0
91. Hilber I, Blum F, Leifeld J, Schmidt HP, Bucheli TD. Quantitative Determination of PAHs in Biochar: A Prerequisite To Ensure Its Quality and Safe Application. *J. Agric. Food Chem.* **2012**, *60*, 3042–3050. DOI:10.1021/jf205278v
92. Buss W, Mašek O. Mobile organic compounds in biochar—A potential source of contamination: Phytotoxic effects on cress seed germination. *J. Environ. Manag.* **2014**, *137*, 111–119. DOI:10.1016/j.jenvman.2014.01.045
93. Roberts KG, Gloy BA, Joseph S, Scott NR, Lehmann J. Life Cycle Assessment of Biochar Systems. *Environ. Sci. Technol.* **2010**, *44*, 827–833. DOI:10.1021/es902266r
94. Foo KY, Hameed BH. Insights into the modeling of adsorption isotherm systems. *Chem. Eng. J.* **2010**, *156*, 2–10. DOI:10.1016/j.cej.2009.09.013
95. Murphy OP, Vashishtha M, Palanisamy P, Kumar KV. A Review on the Adsorption Isotherms and Design Calculations for the Optimization of Adsorbent Mass and Contact Time. *ACS Omega* **2023**, *8*, 17407–17430. DOI:10.1021/acsomega.2c08155
96. Ho YS, McKay G. Pseudo-second order model for sorption processes. *Process Biochem.* **1999**, *34*, 451–465. DOI:10.1016/S0032-9592(98)00112-5
97. Weber WJ, Morris JC. Kinetics of Adsorption on Carbon from Solution. *J. Sanit. Eng. Div. ASCE* **1963**, *89*, 31–59. DOI:10.1061/JSEDAI.0000430
98. Chen T, Da T, Ma Y. Reasonable calculation of the thermodynamic parameters from adsorption equilibrium constant. *J. Mol. Liq.* **2021**, *322*, 114980. DOI:10.1016/j.molliq.2020.114980
99. Viotti P, Marzeddu S, Antonucci A, Décima MA, Lovascio P, Tatti F, et al. Biochar as Alternative Material for Heavy Metal Adsorption from Groundwaters: Lab-Scale (Column) Experiment Review. *Materials* **2024**, *17*, 809. DOI:10.3390/ma17040809
100. Ji Y, Xu W, Chen A, Du J, Hou S. Porous carbon materials for enhanced carbon dioxide capture toward post-combustion. *Mater. Today Energy* **2025**, *47*, 101746. DOI:10.1016/j.mtener.2024.101746
101. Li J, Pan L, Huang Y, Liu X, Ye Z, Wang Y. Biochar design for antibiotics adsorption via a hybrid machine-learning-based optimization framework. *Sep. Purif. Technol.* **2024**, *348*, 127666. DOI:10.1016/j.seppur.2024.127666